HHS Public Access

Author manuscript

Brain Behav Immun. Author manuscript; available in PMC 2024 January 01.

Published in final edited form as:

Brain Behav Immun. 2023 January ; 107: 165–178. doi:10.1016/j.bbi.2022.10.003.

Altered EEG, Disrupted Hippocampal Long-Term Potentiation and Neurobehavioral Deficits Implicate a Delirium-like state in a Mouse Model of Sepsis

David C. Consoli,

Brittany D. Spitznagel,

Benjamin M. Owen,

Hakmook Kang,

Shawniqua Williams Roberson,

Pratik Pandharipande,

E. Wesley Ely,

William P. Nobis,

Julie A. Bastarache,

Fiona E. Harrison

Vanderbilt University Medical Center, 7465 MRB4, Nashville, TN 37232, USA.

Abstract

Sepsis and systemic inflammation are often accompanied by severe encephalopathy, sleep disruption and delirium that strongly correlate with poor clinical outcomes including long-term cognitive deficits. The cardinal manifestations of delirium are fluctuating altered mental status and inattention, identified in critically ill patients by interactive bedside assessment. The lack of analogous assessments in mouse models or clear biomarkers is a challenge to preclinical studies of delirium. In this study, we utilized concurrent measures of telemetric EEG recordings and neurobehavioral tasks in mice to characterize inattention and persistent cognitive deficits following polymicrobial sepsis. During the 24-hour critical illness period for the mice, slow-wave EEG dominance, sleep disruption, and hypersensitivity to auditory stimuli in neurobehavioral tasks resembled clinical observations in delirious patients in which alterations in similar outcome measurements, although measured differently in mice and humans, are reported. Mice were tested for nest building ability 7 days after sepsis induction, when sickness behaviors and spontaneous activity had returned to baseline. Animals that showed persistent deficits determined by poor nest building at 7 days also exhibited molecular changes in hippocampal long-term potentiation compared to mice that returned to baseline cognitive performance. Together, these behavioral and electrophysiological biomarkers offer a robust mouse model with which to further probe molecular pathways underlying brain and behavioral changes during and after acute illness such as sepsis.

Address correspondence to Fiona Harrison, Vanderbilt University Medical Center, Nashville, Tennessee, USA. fiona.harrison@vumc.org.

Author Contributions: DCC, FEH, JAB, and WPN designed the studies. DCC, BDS, and BMO performed animal electrophysiology and behavioral experiments. HK performed statistical analysis of EEG data. DCC and FEH performed all other statistical analysis. JAB, WPN, SWR, PP, and EWE provided clinical input into experimental design and data interpretation. FEH and DCC were responsible for manuscript preparation and project oversight.

Keywords

Sepsis; Delirium; Neuroinflammation; EEG; Memory; Behavior; Long term potentiation

1. Introduction

Sepsis is defined as a dysregulated host response to infection leading to multi-organ dysfunction (Singer et al., 2016). Of the more than 48 million estimated annual sepsis cases globally, approximately 37 million survivors are then at increased risk for development of cognitive impairments (Rengel et al., 2019; Rudd et al., 2020). Development of delirium in the hospital is among the strongest predictors of development of dementia following recovery from sepsis (Chou et al., 2017; Iwashyna et al., 2010; Pandharipande et al., 2013). Organ dysfunction during critical illness and systemic inflammation drives acute encephalopathy through diverse mechanisms including cardiovascular dysregulation, respiratory failure, microvasculature hypoperfusion, metabolic crisis, toxin accumulation, and endothelial breakdown (Bauer et al., 2018; Hughes et al., 2013; Mazeraud et al., 2016). The acute cerebral pathophysiology defined as sepsis associated encephalopathy manifests clinically as delirium (Remick, 2007; Slooter et al., 2020; Zampieri et al., 2011). The development of sepsis-induced delirium is an independent predictor of mortality and, in those who survive, is predictive of persistent behavioral or cognitive change including the development of dementia and sleep disruptions, particularly in older adults (Atterton et al., 2020; Ely et al., 2004; Iwashyna et al., 2010; Pandharipande et al., 2013; Rengel et al., 2019; Sasannejad et al., 2019; Wolters et al., 2013).

Delirium is typically diagnosed using a clinical assessment tool, the Confusion Assessment Method for the ICU (CAM-ICU)(Ely et al., 2001) that depends on the patient's ability to understand instructions delivered verbally. Delirium as defined by the DSM-5 occurs as a direct consequence of some other medical reason (such as surgery, infection, intoxication), and not must not be due to low arousal (coma) or some other clear cause of cognitive disturbance (e.g. dementia). Disturbances in attention and awareness are typically reported occurring over a relatively short amount of time and may fluctuate according to time of day. To be counted as delirium these changes themselves must not be attributable to other causes such as medication or injury. Attentional change is typically accompanied by some other marker of altered cognition which may be in language, understanding or memory. Rodent models, therefore, have had limited face validity for testing of mechanisms, biomarkers, or therapeutic strategies specifically targeted to delirium. Classic descriptions of delirium include disruptions of awareness and inattention that are associated with generalized slow activity in EEG (Engel and Romano, 1959). EEG has been used as a research tool for decades to study delirium in critically ill patients, culminating in reports of slow-wave dominance, disrupted alpha rhythms, (Atterton et al., 2020; Jacobson et al., 1993; Koponen et al., 1989) and a series of increasingly well-defined EEG abnormalities (Hirsch et al., 2021; Palanca et al., 2017). More recently, our group and others showed that slow-wave EEG activity correlates specifically with delirium severity and is predictive of worse outcomes and long-term cognitive impairment (Kimchi et al., 2019; Nielsen et al., 2019; Roberson et al., 2020). It has previously been noted that higher spectral density calculated

from bispectral EEG (BSEEG) recordings as a ratio between low (3 Hz) and high (10 Hz) frequencies can identify delirium cases from controls, with some decrease in values corresponding to recovery from delirium. The use of a BSEEG score was also predictive of later mortality in sepsis and non-sepsis cases (Shinozaki et al., 2018, 2019; Yamanashi et al., 2021b). A related analysis of EEG data from LPS-treated mice indicated similar changes that were also sensitive to LPS dose. Until recently, similar efforts to measure EEG in rodent models of sepsis have been limited to tethered EEG systems in which animal movement is restricted by the recording apparatus. This approach makes long-term recording difficult and prevents synchronization of naturalistic behavioral assessment and EEG metrics during and following illness (Kimchi et al., 2017; Leavitt et al., 1994; Trzepacz et al., 1992).

In addition to the EEG abnormalities, delirium is characterized by inattention and disorganized thinking. In patients, characterization of these behavioral changes are also dependent on CAM-ICU assessment (Ely et al., 2001). Behavioral changes that reflect the hippocampal dysfunction as observed in patients have been noted in rodent models of sepsis including deficits in hippocampal-dependent contextual fear conditioning, (Hippensteel et al., 2019) a step-down inhibitory avoidance task, (Schwalm et al., 2014) and the radial arm maze (Semmler et al., 2007) from 7 to 90 days after recovery. Aged wild-type mice tested in water maze 3-months post treatment with lipopolysaccharides (LPS) had changes in long term potentiation (LTP) even without robust deficits in memory (Beyer et al., 2020). The 5-choice serial reaction time task (5-CSRTT) was originally introduced to study effects of neuropharmacological manipulation on different aspects of attentional function in rats (Robbins, 2002)(Robbins et al., 1993). The original neuropsychiatric focus was Attention Deficit Hyperactivity Disorder. However, the task has since been adapted to mice and to a range of different genetic, disease and other interventional states including a model of post-operative delirium (R. Velagapudi et al., 2019). Post-surgical testing of attention in the 5-choice serial reaction time task highlighted impairments and slowed responses within 24 hours of surgery suggestive of a delirium-like state (Ravikanth Velagapudi et al., 2019). Other surgical and environmental disruption interventions triggered similar short-term disruption in a set shifting attentional task and other tests of hippocampal memory (Illendula et al., 2020). Nevertheless, such tasks may be confounded by enhanced learning due to chronic food deprivation during training (in the case of operant learning), pain, or lack of motivation due to acute effects of illness, and often include some indicators of decreased level of arousal, which could preclude a true delirium diagnosis.

Our goal was to assess changes in EEG activity, sleep and behavior during acute illness -and short-term recovery using a clinically relevant sepsis model which causes systemic inflammation and organ dysfunction. In mice, sepsis was induced using an intra-peritoneal injection of polymicrobial cecal slurry (CS) that did not require surgery or anesthesia (Bastarache et al., 2021; David C. Consoli et al., 2020; Kerchberger et al., 2019; Meegan et al., 2020; Shaver et al., 2019). We used naturalistic behaviors (spontaneous activity and nest building ability) to avoid the need for long-term pre-training of animals in previous studies and to perform behavioral testing during and immediately following the 24 hour sickness period and up to 7 days following CS treatment. To measure attention during illness in mice, we utilized a novel implementation of a passive behavior task that measures pre-pulse inhibition of the startle response as a pre-attentional process. The use of implanted

EEG telemeters permitted longer term assessment of freely mobile mice in the home cage enabling us to define the EEG signature of acute encephalopathy in rodents reflective of delirium, and its consequences. To connect persistent cognitive impairments following recovery with synaptic function, we performed *ex vivo* hippocampal electrophysiology to measure changes in long-term potentiation following illness. Together, these studies outline a comprehensive mouse model of sepsis associated encephalopathy that closely resembles patient delirium and subsequent cognitive decline that may be useful for testing novel hypotheses and interventions.

2. Methods

2.1 Cecal slurry model of sepsis

To model sepsis-associated encephalopathy in mice, we utilized a polymicrobial cecal slurry (CS) method of sepsis induction as previously described (Consoli et al., 2020; Kerchberger et al., 2019; Meegan et al., 2020; Shaver et al., 2019). C57Bl/6J donor mice were obtained at six weeks of age from Jackson Laboratory (#000664) and euthanized within 7 days of arrival. Cecal contents were collected and resuspended in 5% dextrose at 80 mg/ml, then filtered through a 100 μm filter. Aliquots were stored at −80°C until used.

All other mice were bred in house from C57Bl/6J mice originally obtained from Jackson Laboratory. Mice were maintained on a consistent 12-hour light/dark cycle (lights on at 06:00) throughout lifetime and experimental study. For EEG studies, mice at 10–12 weeks of age underwent telemetry device implantation surgery. Approximately 5–7 days following surgery, mice were treated with CS (1.5 mg/g; i.p.) or the vehicle (Veh, 5% dextrose, i.p.). For LTP studies, mice received CS treatment at 8–10 weeks of age. At 8 and 20 hours following initial injection, all mice received antibiotics and fluid resuscitation in the form of 1.5 mg imipenem (IPM) stabilized in cilastatin and suspended in 300 μl of 0.9% NaCl saline (Steele et al., 2017) to increase survival in CS treated mice. Imipenem is a carbapenem class beta lactam antibiotic that has no association with delirium severity during critical illness (Grahl et al., 2018). For EEG studies, mice were singly housed following surgeries and for all other studies, control and treated mice were equally distributed across cages with 2–5 mice per cage. All mice were provided supplemental nutrition on the floor of the cage (DietGel 76A, Clear H_2O) following initial injection and throughout recovery up to 48 hours post injection to promote survival. The mice were monitored every 4–8 hours for 24 hours during onset of illness and recovery for body weight and evaluation of Clinical Sickness Score (Consoli et al., 2020; Kerchberger et al., 2019; Meegan et al., 2020; Shaver et al., 2019). The score is determined by response to finger poke (4 - normal, 3 - decreased, 2 - severely decreased, 1 - minimal response), signs of encephalopathy (4 - normal, 3 - tremors or staggering, 2 - twisting movements, or 1 - turning), and general appearance (score is decreased by 1 for each display of piloerection, periorbital exudates, respiratory distress, or diarrhea).

Twenty-six mice underwent telemetry device surgery and recording across four separate cohorts. One male and one female were excluded, because they died during illness prior to completion of recovery trajectory. Two male and one female were excluded, because they did not exhibit sufficient signs of behavioral illness (Clinical Sickness Score was never

<10 out of a maximum of 12). The final 21 mice are depicted in the figures representing 11 males (4 vehicle and 7 CS treated) and 10 females (4 vehicle and 6 CS treated). The LTP study used 30 mice across five separate cohorts. Three male and two female that did not exhibit sufficient signs of illness, and one female mouse that died during illness were excluded from all analyses. The remaining 24 mice are depicted in the figures representing 13 males (6 vehicle and 7 CS treated) and 11 females (5 vehicle and 6 CS treated). All experimental protocols using live mice were reviewed and approved by the Vanderbilt Institutional Animal Care and Use Committee.

2.2 EEG Telemetry

Telemetry Device Implantation Surgery.—To record electroencephalogram (EEG) activity in mice while minimizing disturbance to normal behavior, we utilized a wireless EEG telemetry system (PhysioTel HD-X02; Data Sciences International, DSI, St. Paul, MN) as previously described (Gould et al., 2020). In brief, mice were anesthetized (isoflurane 2–5%) and a wireless telemetry device was implanted in each mouse subcutaneously between the left shoulder and hip according to the manufacturer's protocol. Four wires (0.3 mm diameter helix of stainless-steel coils protected with silastic coating 0.63 mm in diameter) connected the device to the recording and reference sites in the neck muscle for electromyograph (EMG) recording and to the skull for EEG recording. EEG leads were inserted into two burr holes 1-mm in diameter exactly +1.0 mm anterior-posterior, −1.0 mm medial-lateral from bregma for reference and −3.0 mm anterior posterior, +3.0 mm medial-lateral from bregma for recording. The skull was covered with dental cement and the incision site was sutured. Mice received analgesic (ketoprofen, 10 mg/kg, i.p.) immediately and at 24 hours following surgery for at least 48 hours of analgesic coverage. Mice were allowed 4–6 days of recovery prior to acquisition of baseline data.

Telemetry Device Data Acquisition.—Following telemetry device implantation surgeries, individual cages of singly housed mice were placed on a PhysioTel receiver plate (model RPC-1) that transmitted data in real time from the wireless implant to a computer using the MX2 data exchange matrix and Dataquest ART software (DSI, St. Paul, MN). Data were collected using Ponemah Physiology Platform version 5.20 software (DSI, St. Paul, MN). Single channel EEG and EMG were sampled at a rate of 500 Hz, and activity counts were sampled at 50 Hz. Video (20 frames/sec) of each mouse was recorded using Axis cameras (M1145-L) and MediaRecorder 2.6 (Noldus) and synchronized to physiologic measurements. Approximately one week following completion of surgeries and prior to CS or vehicle treatment, 24 hours of baseline telemetry data including EEG, EMG, and activity were recorded for all mice. After CS treatment or vehicle injection, telemetry data were collected in 24 hour increments up to 72 hours post injection and then again 7 days post injection for a total of five, 24-hour periods as depicted in Figure 1A.

Prior to injections, mice were briefly anesthetized with isoflurane to avoid displacing the EMG and EEG leads during handling, requiring temporary removal of the mice from the plate reader for less than one minute. During Clinical Sickness Scoring, mice were scored in their cages on the receiver and weighed by removal from the cage onto a scale near the plate reader with minimal disruption of data acquisition.

Telemetry Device Data Analysis.—Telemetry data were analyzed using NeuroScore (version 3.3.0, DSI, St. Paul, MN). To determine global changes in EEG independent of behavioral vigilance state, spectral power band analyses separated the EEG signal into relative power percentages using 10 second epochs across different frequency bands (delta 0.5–4 Hz, theta 4–8 Hz, alpha 8–12 Hz, sigma 12–16 Hz, beta 16–24 Hz, and gamma 24–50 Hz). The averaged power percentages for each hour were normalized to the average baseline value. The theta ratio is reported as relative theta power divided by relative delta power normalized to the average baseline value. For telemetry activity data, the maximum activity count per 10 second epoch was determined, and the sums of activity counts per hour and total activity per 24-hour period are reported.

To determine changes in EEG within behavioral vigilance states, data were visualized and scored within 10 second epoch windows according to DSI instructions for Sleep Scoring in Neuroscore (Gould et al., 2020). Periodograms ranging from 0 to 25 Hz were viewed in 10 second epochs alongside continuous plots of EEG theta ratio, EEG number of crossings, EEG and EMG raw traces, and activity counts. The behavioral state for each 10 second epoch was scored as non-rapid eye movement (NREM, slow-wave sleep), REM (paradoxical sleep), or wake. High delta power, low theta ratio, low EMG muscle tone, and low activity counts were scored as NREM. High theta power and theta ratio, low number of crossings, low EMG muscle tone, and low activity were scored as REM. High EMG muscle tone and high activity counts with low to medium delta and theta power were scored as wake. Micro-wakes and quiet wake were included as wake. Sleep stages were scored for one hour at the same time of day (17:00–18:00) at baseline (Day 0), during illness (Day 1), following acute recovery (Day 2), and following long-term recovery (Day 7). The relative power for each 1 Hz frequency within each sleep stage was averaged and reported.

A clinically derived bispectral EEG (BSEEG) score has been shown to be predictive of delirium and associated later mortality in septic and non-septic critically ill patients (Shinozaki et al., 2018, 2019; Yamanashi et al., 2021b). The BSEEG score is based on a ratio of low (3 Hz) to high (10 Hz) frequencies. We calculated this ratio for our data set at baseline, 8 hours, 48 hours, and 7 days, with data divided according to sleep state (NREM, REM and Wake).

2.3 Behavioral Assessment

2.3.1 Nest Building.—

Nest building was assessed overnight the night prior to CS treatment, after Day 2 (approximately 36–48 hours post CS) and on the 7th night following CS (Figs. 1 and 4). Mice were singly housed overnight with two squares of pressed cotton nestlet material (AnCare Ltd.) weighing a total of 5.0 g stacked in the center of each cage. Nests were scored the following morning based on three primary criteria adapted from (Deacon, 2006)(Table 1) including i) presence of a clear nest site, ii) extent of nestlet shredded and utilization of un-shredded nestlet (if less than 50% was shredded), and iii) nest height. If nest criteria were deemed between two score designations scores were made with 0.5-point increments. Nests were scored with a combination of ‘live’ scoring which permits a better visualization of the 3 dimensional nature of the nest, with secondary scoring occurring from photographs. Treatment groups were not marked on cages, and nests

were scored blind to treatment group. Nest building was never performed at times when mice were demonstrably sick. Graphical representations of nests of varying complexity are illustrated in Figure 1B. Nest building score at day 7 was used to subdivide mice for post-recovery analyses. CS treated mice that had nest building scores at day 7 equivalent to pre-CS levels (score > 3.0) were designated “recovered” whereas mice that built poor nests (score < 3.0) were placed in the “persistent deficits” group. The criteria were based on the lowest score observed in vehicle treated mice in Experiment 1 and applied to all experimental groups for consistency.

2.3.2 Locomotor Activity – Home cage.—Activity within the home cage was recorded continually and automatically according to the manufacturer protocol based on the position of the telemeter on the baseplate whenever the telemeter was turned on.

2.3.3 Locomotor Activity – Novel Environment.—Open-field activity was recorded through the breaking of infrared beams using standard locomotor activity chambers (approx. 30 × 30 cm, ENV-510; MED Associates, Georgia, VT, USA). Activity was measured on day 2, approximately 48 hours after CS injection and on day 7 (Fig. 4). Total activity travelled during the 30-minute trial is reported. An ‘open field’ analysis was performed to compare time spent within the center versus the edge during the first 5 mins. of each session, with each zone comprising approximately 50% of the total surface area. Activity chambers were thoroughly cleaned between each animal with a 10% ethanol solution.

2.3.4 Pre-pulse Inhibition of Acoustic Startle Response.—PPI was measured 24 hours prior to CS injection, and 4 and 8 hours following treatment (Fig. 4). Mice were placed in a small, clear acrylic animal holder, cylindrical in shape and mounted on a white acrylic base. The holder was secured to a startle platform detector housed within an acoustic chamber insulated with 2 cm sound attenuating foam (ENV-022S, MED Associates). Various startle and pre-pulse stimuli were delivered using Startle-PPI Pro Series software (SOF-826, MED Associates). Testing consisted of six different trials (null, 0 dB; startle only, 120 dB; pre-pulse at 72, 76, 82, 88 dB each followed by startle at 120 dB) repeated nine times in a pseudo-random order for a total of 54 trials. The mice were allowed an acclimation period of 5 minutes before trials began, and time between trials was 30 seconds. In trials with a pre-pulse, the pre-pulse stimulus was delivered 50 ms before startle stimulus. The highest and lowest values for each trial type were excluded, and the average response per trial type was determined. The percent pre-pulse inhibition was calculated at each pre-pulse amplitude using the difference between the pre-pulse trials and the startle only trial.

2.4 Long-Term Potentiation

Hippocampal slices were prepared from 8–10-week-old mice treated with CS or Veh. Mice were briefly anesthetized and then sacrificed by decapitation. The brain was quickly removed into an ice-cold solution of sucrose-rich artificial cerebrospinal fluid (aCSF) containing 85 mM NaCl, 2.5 mM KCl, 1.25 mM NaH_2PO_4, 25 mM $NaHCO_3$, 75 mM sucrose, 25 mM glucose, 10 μM DL-APV (NMDA antagonist), 100 uM kynurenate, 0.5 mM sodium L-ascorbate, 0.5 mM $CaCl_2$, and 4 mM $MgCl_2$ oxygenated and equilibrated

with 95%O_2/5%CO_2 and titrated to a pH of 7.4. The brain was mounted on a slicing stage ventral side up, and 300 μm horizontal slices were prepared using a Leica VT-1200S vibratome (Leica Biosystems) in sucrose-aCSF. The coronal slices were micro-dissected along the sagittal plane into two halves before transferring to a holding chamber containing sucrose-aCSF warmed to 32°C that slowly returned to room temperature over the course of 30 minutes. Slices were then transferred to a second holding chamber containing room temperature aCSF containing 125 mM NaCl, 2.4 mM KCl, 1.2 mM NaH_2PO_4, 25 mM $NaHCO_3$, 25 mM glucose, 2 mM $CaCl_2$, and 1 mM $MgCl_2$ oxygenated and equilibrated with 95%O_2/5%CO_2 and titrated to a pH of 7.4. Slices were maintained under these conditions until transferred into a submerged recording chamber (Scientifica SliceScope Pro 2000, Scientific UK) flowing warmed (in-line heater temperature set at 36°C) oxygenated aCSF at approximately 6 ml/min.

Field excitatory postsynaptic potentials (fEPSPs)(Abrahamsson et al., 2016; Wilcox et al., 2021a) were recorded by stimulating along the Schaffer collaterals in the stratum radiatum and recording the response from the Cornu ammonis 1 (CA1) region of the hippocampus at a rate of 0.05 Hz (Fig. 5A). An input-output relationship was determined for each slice, plotting the peak amplitude of the fiber volley against the slope of the fEPSP. For LTP experiments, the baseline recordings used a stimulus intensity that produced ~40% of the maximum response and were recorded for at least 20 min before tetanizing the slice. LTP was induced using theta-burst stimulation (5 bursts at 100 Hz, repeated at 5 Hz over 5 seconds, with each tetanus including four of these burst trains separated by 10 seconds, totaling 100 bursts). Experiments in which the fiber volley amplitude changed by >20% post-tetanus were discarded. Recordings were continued for at least 60 mins post-tetanus. The magnitude of LTP was measured in the last 5 minutes of the 60 minutes post tetanus recording. There were 5–8 slices in each group from 2–3 mice.

2.5 Statistics

Data shown in figures and text are reported as mean +/− S.E.M. Bar graph data were analyzed using GraphPad Prism (version 9.1.1). Proposed N for all experiments was calculated based on previous data from our labs (Consoli et al., 2020; Hedrick et al., 2017; Wilcox et al., 2021b) in the sepsis model, EEG outcomes, behavior and LTP studies. All groups were equally balanced male and female mice, and analyses were first run with sex as a fixed variable. There were no significant meaningful differences according to sex, thus data were collapsed and analyzed together. All data were first checked for normality with an Anderson Darling test (alpha = 0.05), and all data with normal Gaussian distribution were subsequently analyzed using parametric statistical analyses. Nest building data were not normally distributed and were instead analyzed using the non-parametric Kruskal-Wallis test, and the Kruskal-Wallis statistic (KW) is reported. Following significant results, nest building scores for each group were compared with Dunn’s test for nonparametric comparisons. Data acquired from locomotor activity chambers were analyzed using a two-way repeated measures ANOVA with time and treatment as independent variables. Following significant results, activity data were compared to baseline activity levels using a Dunnett’s multiple comparisons test. Periodogram data were analyzed using an ordinary two-way ANOVA with treatment as an independent variable and frequency as dependent

variable. Tukey's multiple comparison test was used to compare differences between treatment groups within each frequency. PPI data were analyzed using a two-way repeated measures ANOVA, with treatment and pre-pulse amplitude as independent variables. To compare means across vehicle and CS treated mice specifically within each pre-pulse amplitude, treatment groups were compared using a Šídák's multiple comparisons test. LTP data were analyzed by Univariate ANOVA (FV/EPSP ratio, FV pre-post ratio, LTP percent change from baseline), RM-ANOVA (paired pulse ratios at baseline and post-TBS), and Pearson r correlation (final baseline EPSP slope and nest building score).

We conducted statistical analyses of EEG theta ratio and power bands using R Statistical Software version 4.0.3 (R Foundation for Statistical Computing, Vienna, Austria). To assess the difference in the change of each EEG metric over time between CS and vehicle during the first and final 24-hour periods following injection, we used a linear mixed-effects model with a random intercept in which the EEG metric was the dependent variable and the group indicator (i.e., CS vs. Veh), time, and the interaction term between the group and time were the explanatory variables. Because the EEG data did not follow a simple linear trend (i.e. a straight line) over time we employed statistical techniques to properly model the non-linear trends in our models. We employed natural cubic splines of time variables which offers the most flexibility within the data. We further employed an autoregressive order one (AR(1)) approach to control for the fact that since we were modelling continuous change over time any single observation is typically highly correlated with its previous and subsequent observation. Statistical significance (p-value < 0.05) was tested by comparing the model with the interaction terms to the model without them by a likelihood ratio (LR) test. For each model, we tested for the effect of sex on the association of interest, i.e., the association between Theta ratio and the interaction between time and group (e.g., CS vs. Veh). There was no significant sex effect in any of the models.

3. Results

3.1 CS treatment causes both acute and persistent deficits in nest building

Throughout EEG data acquisition, we used nest building (designated NB in figures) to measure changes in cognitive ability following recovery from CS treatment (Fig. 1A–B). All CS treated mice showed similar illness trajectory by Clinical Sickness Score evaluation (p's>0.2912, Fig. 1C) based on responsiveness, signs of encephalopathy, and appearance. Nest building scores did not vary in vehicle treated mice up to Day 7 following injection ($KW=1.269$, $p=0.5302$), but nest building scores were significantly decreased following illness in CS treated mice (KW's>11.26, p's<0.0009). These deficits were most apparent on Day 2 following illness when all mice performed poorly and were more variable on Day 7, which permitted subdivision of CS-treated animals into two distinct groups termed "recovered" and "persistent deficits" based on nest building score at 7 days. Differential long-term recovery in CS-treated mice was distinguishable on Day 7 ($p=0.0072$) but the two groups did not differ on Day 2 ($p>0.99$). This separation of CS treated mice based on long-term recovery was utilized throughout remaining data analysis to explore individual metric contributions to long-term cognitive deficits.

3.2 Activity returned to normal following CS treatment regardless of nest building deficits

Total activity per day was compared across groups and time. Changes in activity of CS treated mice during and following illness drove a significant interaction between time and treatment ($F_{8,72}$=9.691, p<0.0001). As expected, total activity did not change in vehicle treated mice throughout the experiment (p's>0.6987), and all CS treated mice had decreased activity during illness on Day 1 (p's<0.0001). Hypoactivity in CS treated mice persisted following acute recovery until Day 3 (p's<0.0033), and by Day 7 activity had fully returned to baseline levels (p's>0.9217) in all groups (Fig. 1E). Closer analysis of activity per hour within light/dark cycles showed normal activity across all groups at baseline were greatly disrupted during illness on Day 1 and following acute recovery. Normal activity and circadian rhythms were observed in all groups by Day 7 regardless of nest building outcome on Day 7 (Fig. 1F). Normal activity levels on Day 7 in all CS treated mice indicated that nest building deficits on Day 7 were not due solely to persistent hypoactivity.

3.3 CS treatment causes EEG slowing during illness

To compare global changes in EEG frequencies during and following illness, we first examined the average theta ratio per hour throughout the experiment. During illness, CS treated mice displayed a dramatic decrease in theta ratio that persisted until mice were no longer showing overt sickness behaviors at approximately 24 hours (LR=99.1052, p<0.0001, Fig. 2A). Overall trajectory of theta ratio during the first 24 hours of illness was marginally different between CS groups depending on persistent nest building deficits (LR=7.7511, p=0.0514). Theta ratio was not significantly different between any groups on Day 7 (LR=6.7642, p=0.0798).

3.4 EEG Power band analysis

Global changes in EEG signatures were further investigated by dividing the data into six functionally distinct power bands of differing frequency ranges. Average power percent per hour was reported for delta (0.5–4 Hz), theta (4–8 Hz), alpha (8–12 Hz), sigma (12–16 Hz), beta (16–24 Hz), and gamma (25–50 Hz) (Fig. 2B–G). Changes in power band composition in CS treated mice were most apparent from 0–24 hours following injection. During illness onset, delta power increased (LR=104.6962, p<0.0001, Fig. 2B) as theta power decreased (LR=78.8804, p<0.0001, Fig. 2C) compared to vehicle. Following illness, delta power returned to baseline as theta power increased (Fig. 2B–C). Increased theta power gradually returned to normal levels by Day 3. Alpha power decreased during illness and returned to normal upon recovery by 24 hours (LR=54.8937, p<0.0001, Fig. 2D). There were no changes in sigma power during illness (LR=4.3151, p=0.2294, Fig. 2E). Higher frequency ranges including beta and gamma power were increased during illness (Beta: LR=12.1489, p=0.0069; Gamma: LR=27.8134, p<0.0001 Fig. 2F–G). No significant differences in EEG power were observed at the 7 day timepoint (LR's<2.9358, p's>0.4016).

Similar to previous reports on BSEEG the 3 Hz/10 Hz ratio was clearly increased in the sick animals in the 24 hours following CS injection, however, this value was similarly unable to further differentiate between the recovered and persistent impaired groups when compared according to nest building ability on day 7 (Supplemental Figure 1).

3.5 Periodograms within Sleep Stages show generalized EEG slowing during illness.

Given the significant sleep disruptions observed in ICU patients relating both to illness, pharmacological treatment and other medical interventions (Illendula et al., 2020; Mart et al., 2020; Opp et al., 2015) we investigated the effects of CS treatment on sleep by analyzing EEG power changes specifically within mouse behavioral sleep stages. Using the same EEG dataset, we generated spectral periodograms to visualize and compare changes in EEG within sleep stages (Fig. 3A). The timeframe shown is hour 7–8 (17:00–18:00) following vehicle or CS injection, during peak critical illness, prior to antibiotic injection, and just prior to light-cycle change. EEG activity in CS treated mice was broadly dominated by slower EEG frequencies during illness. Slow-wave dominance is even more apparent when these periodograms were compared across sleep stages to vehicle treated mice. Vehicle treated mice showed normal variation in sleep stages by exhibiting wake, NREM, and REM sleep stages within each hour scored. Periodograms scored as NREM sleep and wake for CS treated groups both had greatly increased delta power (<4 Hz) that did not resemble normal NREM sleep and wake in vehicle treated animals (Fig 3Biv NREM p's<0.0095; Fig. 3Bvi wake p's<0.0029). CS treated mice showed increased atypical NREM sleep and decreased wake with no observable REM sleep during illness (Fig. 3A, Biv-vi, C).

Further sleep disruption was observed up to 7 days post CS through subtle changes in power frequencies across sleep stages following illness. During the periods scored at 32 and 152 hours post CS treatment, immediately prior to initiation of the nest building tasks, CS treated mice had altered NREM and REM sleep, and wake periodograms (Fig. 3Bvii-xii). During wake, CS treated mice had decreased delta power and increased theta power compared to vehicle treated mice (p's<0.0128). Most notably, during REM in the long-term recovery period (152 hours), CS treated mice with persistent deficits had significantly decreased theta power compared to CS mice who recovered (Fig. 3Bxi, p=0.0313).

3.6 Elevated PPI implicates hypersensitivity to stimulus.

In a second experiment using a separate set of animals, we again utilized nest building to determine which mice had persistent post sickness cognitive deficits on Day 7 and further tested exploratory activity in locomotor activity chambers in the same mice (Fig. 4A). During the acute illness phase (4–8 hours post CS injection), we measured pre-pulse inhibition (PPI) of the startle response as a behavioral measure of attention and awareness during illness. For initial analysis, data for all mice were collapsed into vehicle or CS treated groups because some mice were euthanized prior to 7 days when the final nest building test was performed. No changes were observed in startle response to the 120 dB tone (no pre-pulse) during illness (Time: $F_{2,42}$=2.718, p=0.0776; Treatment: $F_{1,21}$=0.2477, p=0.6238, Fig. 4B). At 4- and 8-hours post treatment, CS treated mice showed an unexpected increase in PPI (Fig. 4C, 4E 4 hrs: Treatment, $F_{1,22}$=6.992, p=0.0148; 8 hrs: Treatment, $F_{1,22}$=15.95, p=0.0007) indicating a greater inhibition of startle response reflecting a likely hypersensitivity to the pre-pulse stimulus during illness. This effect was exaggerated when compared as a change from baseline measures for each mouse (Fig. 4D, 4F 4 hrs: Treatment, $F_{1,22}$=16.08, p=0.0006; 8 hrs: Treatment, $F_{1,22}$=15.01, p=0.0008). However, when groups were separated post-hoc based on nest building score on day 7 (for those animals that were

not euthanized until day 7), there were no significant differences in PPI response between CS groups with differential nest building outcome (p's>0.9991).

Distribution of nest building scores recorded in this experiment resembled those observed previously in mice that had undergone telemetry implant surgeries. CS treated mice showed poor nest building ability on Day 2 following illness (KW=9.806, p=0.0006), but by Day 7 approximately 50% of the mice had scores greater than 3 indicating some recovery while the remaining animals showed a persistent impairment (KW=8.723, p=0.0009, Fig. 4G). Activity data also recapitulated findings from the previous experiment, showing significant effects of time driven by hypoactivity on Day 2 ($F_{2,29}$=4.477, p=0.0202). Activity returned to normal exploration levels on Day 7 regardless of Day 7 nest building outcome (p's>0.3502, Fig. 4H). Despite changes in overall activity level, time spent exploring the central 50% of the chamber area did not differ according to treatment either at Day 2 or Day 7 (Day 2 t(16)=1.029, p=0.318; Day 7 $F_{(2,7)}$=0.857, p=0.464, Fig. 4I–J).

3.7 Deficits in Long-Term Potentiation implicate long-term cognitive deficits following CS treatment.

To support the hypothesis that nest building deficits are reflective of cognitive impairment rather than solely due to sickness behaviors, we measured long-term potentiation (LTP) in mice that recovered from CS treatment at 2- and 7-days post injection by recording local field excitatory post-synaptic potentials (EPSPs) in ex-vivo hippocampal slices before and after theta-burst stimulation (Fig. 5A–B). We observed normal input-output responses and fiber volley to excitatory post-synaptic potential (EPSP) relationships in the slices (Fig. 5C–E, Time and Treatment, F's<2.022, p's>0.1449). LTP was decreased by roughly 50% in CS treated mice on Day 2 following illness (p=0.0229, Fig. 5F–G). On Day 7, mice that had recovered nest building ability also showed recovered LTP (p>0.99, Fig. 5F–G), however, mice with persistent nest building deficits on Day 7 showed deficits in LTP (p=0.0056, Fig. 5F–G). The magnitude of LTP observed significantly correlated with its corresponding nest building score prior to sacrifice (Fig. 5H, p=0.0103). We observed no changes in paired pulse ratios between groups that would implicate LTP differences driven by alterations in vesicular readily releasable pool (Fig. 5I, F's<06069, p's>0.4451).

4. Discussion

Difficulty measuring behavioral deficits in mice during critical illness and recovery, and a lack of reliable biomarkers for delirium have previously limited preclinical studies of delirium and its correlation with poor cognitive outcomes. Using an innovative combination of behavior and electrophysiological techniques, we present an animal model that quantifies delirium-like mental status in mice. Although others have previously reported changes in EEG following treatment with LPS (Yamanashi et al., 2021a), these were not combined with behavioral outcomes, sickness measures or other molecular markers of damage. We observed dramatic decreases in theta ratio during illness (Fig. 2A) indicating a shift towards slow-wave delta EEG activity confirmed by individual power band analyses (Fig. 2B–G). Similar slow-wave EEG activity is well-documented in delirious patients and is related to cognitive deficits following illness (Engel and Romano, 1959; Kimchi et al., 2019; Mart et

al., 2020; Roberson et al., 2020). We also observed global decreases in alpha power during illness (Fig. 2D), suggesting decreases in active attention. In humans, regular alpha rhythm is a marker of normal responsiveness and is disrupted in delirium (Hirsch et al., 2021; Jacobson et al., 1993; Mulkey et al., 2019). Such changes contribute to the potential utility of calculating delirium relevant scores from EEG data in critically ill patients (Shinozaki et al., 2019, 2018; Yamanashi et al., 2021b).

Delirious patients typically exhibit markedly decreased beta power relative to controls, (Hirsch et al., 2021) and patients with preserved higher-frequency activity including beta power have lower incidence of delirium (Nielsen et al., 2019). The BSEEG score calculated as a ratio of 3 Hz to 10 Hz frequencies (delta/alpha) is also able to discern delirium in patient populations and LPS-induced sickness and neuroinflammatory changes in mice (Shinozaki et al., 2019, 2018; Yamanashi et al., 2021b, 2021a). Surprisingly, we observed elevations in beta and gamma powers in CS treated mice during illness (Fig. 2F–G). Elevated beta frequencies are observed in sedated patients due to sedative-hypnotic drugs, particularly barbiturates and benzodiazepines (Satapathy et al., 2019; Van Lier et al., 2004). Paradoxically, higher beta activity has also been observed as a marker of alertness (Kamiński et al., 2012) stress, anxiety, and arousal (Abhang et al., 2016; Satapathy et al., 2019). Our CS-treated mice with long-term recovery of cognitive function showed higher beta activity levels during illness than those that did not recover. We postulate that the differences in cognitive outcomes between the groups could be related to greater beta activity during illness indicating greater levels of alertness. This explanation would suggest a greater arousal during illness, indicated by greater relative beta power, is associated with better protection against protective of long-term cognitive damage regardless of the extent of overall EEG slowing. This finding may indicate that for some animals the degree of acute encephalopathy was less severe, allowing them to maintain a larger proportion of wakefulness.

During illness, CS treated mice showed profound changes in sleep with periodograms that were dramatically shifted towards slower (delta, 0.5–4 Hz) frequencies and did not resemble normal wake or sleep (Fig. 3). Due to these dramatic shifts, CS treated mice showed no identifiable REM sleep during illness, atypical NREM sleep, and decreased wake consistent with another study of sleep following cecal ligation and puncture to induce sepsis in rats (Baracchi et al., 2011). Although this was classified as NREM sleep, it may be that this state more directly reflects the distorted sleep/wake patterns observed in delirium. Atypical sleep is commonly observed in humans during critical illness both as a result of illness and of treatment and medical intervention and monitoring (Drouot et al., 2012; Watson et al., 2013) and can also be observed in mice following LPS injection (Yamanashi et al., 2021a). Following illness, at both the acute and long-term recovery timepoints we observed decreased theta power intensity during REM sleep, suggesting that sleep may be perpetually altered following illness. Disruptions in normal sleep-wake cycles as well as sepsis due to cecal ligation and puncture triggered neuroimmune dysregulation and both sleep and illness may thus independently contribute to lasting cognitive deficits (Opp et al., 2015). Our data also support the idea that a lack of normal restorative REM sleep may contribute to the persistent deficits based on data from the nest building task. We did not, however, quantify sleep stages continuously across the experimental time point. Although others have

also observed sex differences in sleep patterns in C57Bl/6 mice, these were greater in mice housed under 14:10 h light cycle conditions, and were also magnified by stress and sleep deprivation (Choi et al., 2021; Koehl et al., 2006; Paul et al., 2006). We did not observe differences in sleep patterns between male and female mice at baseline or in response to CS treatment, however, it is possible that subtle differences were masked by the very large effect of sepsis. It is also important that future studies are designed to permit comparisons between male and female mice and also to take into account differences caused by light cycle and other housing conditions.

At 8 hours after CS injection, and immediately following antibiotic administration, beta and gamma power were acutely and temporarily noticeably decreased from the otherwise elevated levels that were observed within 2 hours of CS treatment. Delta and theta were marginally increased following the antibiotic treatment. These alterations following injection were contrary to what we expected, because interacting with a sick mouse should intuitively increase arousal, illustrating the complexity of the relationship between beta power and arousal/behavior. Subsequent influence of antibiotics including comprehensive lysis of bacteria or indirect cerebral drug interactions could contribute to the raising of beta and gamma and dropping of excess delta and theta. Increased LPS accumulation and inflammatory signaling could further decrease arousal driving these observations. Imipenem is a beta-lactam antibiotic belonging to the class of carbapenems, which have a proconvulsant nature through inhibitory receptor antagonism that could drive changes in EEG or LTP (Miller et al., 2011). However, we did not observe any strong EEG or LTP changes in control mice which also received antibiotics. Nevertheless, differences in drug concentrations are possible during illness due to impaired renal function in septic mice. Changes in magnitude of diffuse slow wave activity are indeed sensitive to dose of LPS, and also to the age of the animal with similar changes in EEG recorded at lower doses of LPS in 19 month old compared to 3 month old mice (Yamanashi et al., 2021a). It is possible that in mice with renal failure secondary to sepsis, a carbapenem could contribute to EEG abnormalities that impair learning and hippocampal LTP. This potential mechanism of action should be investigated in future studies and would have important implications for the therapeutic mechanisms of long-term cognitive impairment in septic patients receiving antibiotics.

PPI is a behavioral phenomenon that relies on the ability of the central nervous system to filter out irrelevant stimuli which is required for selective or focused attention (Gómez-Nieto et al., 2020). Although different from conscious attention, this task requires automatic and attentional processes in order to successfully employ sensorimotor gating mechanisms. PPI is sensitive to behavioral states such as anxiety, pharmacological modification, and age and is therefore considered to require neural plasticity and attention (Li et al., 2009). Although we did not observe any significant differences in sensitivity to the 120 dB acoustic tone during illness in CS treated groups in the PPI task, we saw increased PPI potentially reflecting heightened arousal or responsiveness to the pre-pulses in PPI trials. Patients with delirium often present hypersensitivity as restlessness or agitation (Ely et al., 2001; Sessler et al., 2002). Decreased PPI is commonly observed in schizophrenic patients relative to healthy controls (Mena et al., 2016) and is associated with prefrontal cortical dysfunction (Hammer et al., 2013; Kumari et al., 2003). Contrary to our initial predictions, during illness

we found elevated PPI, indicating hypersensitivity to the pre-pulse stimulus that may be indicative of a hyperadrenergic state (Hinson and Sheth, 2012). This would further explain elevations in beta and gamma powers relative to controls. Elevated PPI has been observed in children with autism spectrum disorder and attributed to high stress and anxiety (Madsen et al., 2014). Contributions of hyperadrenergic signaling to long term cognitive deficits varies across different mouse models of sepsis (Field et al., 2012; O'Neill et al., 2021). If hypersensitive PPI is indicative of a hyperadrenergic state that correlates with higher beta and gamma powers, this model would suggest that proper adrenergic regulation could be protective of later cognitive dysfunction.

Nest building ability is a hippocampal dependent task associated with executive function and sometime likened to tasks of daily living in humans. Performance on this task is also impaired in a number of animal models of aging, cytotoxic hippocampal lesion, neurodegeneration and injury (R. M. Deacon, 2006; Deacon and Rawlins, 2002; Deacon et al., 2002; Janus et al., 2015; Ritzel et al., 2020; Walker et al., 2017) that includes both cognitive and non-cognitive factors for strong performance. Importantly, disruption was persistent in a mouse model of stroke suggesting that it can be used in a long-term and repetitive manner that is sensitive to persistent damage and recovery (Yuan et al., 2018). Neurocognitive deficits assessed by decreased nest building ability were supported by deficits in hippocampal LTP, an important molecular foundation of learning and memory (Lynch, 2004). We found similar deficits in LTP in our CS model of sepsis as those reported in two other mouse models of sepsis using lipopolysaccharide and cecal ligation and puncture 7 days following acute illness (Hippensteel et al., 2019). One weakness of our approach was the relatively low number of mice used for the LTP experiments (up to n=3) that might have decreased variability within groups, although these are not atypical for this approach and the number of slices used was sufficient for appropriate analysis. We used an 'open field' analysis as a measure of anxiety like behavior on entering a novel context. Although overall exploratory activity levels differed with treatment and recovery, proportionally the time spent exploring the center versus edge of the locomotor activity chambers did not vary among groups. Nevertheless, given the complex clinical presentation of delirium, future studies may benefit from further extending the range of behavioral tasks used to more fully model changes observed in human populations including measures of attention as well as agitation and anxiety.

Similar to lipopolysaccharide injection CS has several advantages for our study over these other sepsis induction methods including precise dose control of illness severity, and tight temporal control of illness onset all without the need for a surgical procedure and anesthesia but with the added benefit of translationally relevant microbial diversity including live bacteria. Cortical and hippocampal dysfunction are intimately linked via neural disinhibition, (Bast et al., 2017; McGarrity et al., 2017; Moretti et al., 2012) so it is possible that the hippocampal dysfunction we observed in LTP is associated with the cortical dysfunction we observed using EEG. Future studies that assess LTP changes in mice for which there are EEG data will help to clarify this issue. Further, molecular deficits in the hippocampus in sepsis models are reported to require acute brain injury and associated neuroinflammation and do not occur due to systemic inflammation alone (Skelly et al., 2019). Activity levels had not fully recovered at 3 days following CS administration,

which suggests that a combination of both sickness behavior and other motivational factors contribute to altered performance on behavioral tasks. Nevertheless, the combination of behavior and electrophysiological outcomes implicated a cognitive base for some of the deficits seen. This may be particularly true for animals in which LTP and nest building deficits persist at 7 days when spontaneous activity is recovered.

Fewer mice that were utilized in the LTP experiments showed a persistent nest building deficit compared to those observed in the EEG study (24% of mice had observed nest building deficits on Day 7 in the EEG study compared to 13% in the LTP study). Given the extensive research on post-op surgery, delirium, and cognitive decline, (Crosby et al., 2010; Crosby and Culley, 2011; Illendula et al., 2020) the insult of surgery and anesthesia in the EEG study likely contributed to the severity of illness we observed in those mice. Social isolation is known to greatly increase risk of delirium (Kotfis et al., 2020; Pun et al., 2021) and single housing of mice in the EEG study could also have contributed to the severity of any cognitive and behavioral changes, compared to mice in the second study that were housed 3–5 mice per cage.

5. Conclusions

EEG slowing is a strong indicator of delirium and is associated with cognitive deficits following critical illness. The recapitulation of some forms of patient EEG metrics in a mouse model of sepsis demonstrates occurrence of a translationally relevant sepsis associated encephalopathy in mice. Characterization of this acute encephalopathy with EEG and neurobehavioral tasks implicates a delirium-like mental status and will allow the exploration of therapeutic strategies to target this state in preclinical studies. Future studies may also allow identification of factors that promote cognitive resilience in some animals, or specific biological correlates of neuroinflammation and neurometabolism in brain and plasma across the sickness and recovery period. It will also be particularly important to assess how each of these potential biomarkers differs in older animals to contribute to the increasing risk for delirium with age.

Supplementary Material

Refer to Web version on PubMed Central for supplementary material.

Acknowledgements:

This research was funded by NIH grants R01 ES031401-01 to FEH and R01 HL135849 to JAB and RF1 AG075341 to FEH and JAB. This work was supported by grants to WPN from the American Epilepsy Society (Junior Investigator Award), a pilot grant from the National Institute for Neurologic Disease and Stroke Center for unexpected death in epilepsy (SUDEP) center for SUDEP research (CSR), and the Vanderbilt Faculty Research Scholars (VFRS) award. SWR was supported by K23 AG072030. The authors would like to thank Adriana A. Tienda for maintenance of the mouse colony. Jason K. Russell and Rebecca A. Buchanan provided additional assistance in sleep scoring and periodogram analysis.

Abbreviations:

CS	cecal slurry

LTP	long-term potentiation
EPSP	excitatory post-synaptic potential
TBS	theta burst stimulation

References

Abhang PA, Gawali BW, Mehrotra SC, 2016. Introduction to EEG- and Speech-Based Emotion Recognition, Introduction to EEG- and Speech-Based Emotion Recognition. Elsevier Inc. 10.1016/C2015-0-01959-1

Abrahamsson T, Lalanne T, Watt AJ, Sjöström PJ, 2016. Long-term potentiation by theta-Burst stimulation using extracellular field potential recordings in acute hippocampal slices. Cold Spring Harbor Protocols 2016, 564–572. 10.1101/pdb.prot091298

Atterton B, Paulino MC, Povoa P, Martin-Loeches I, 2020. Sepsis associated delirium. Medicina (Lithuania). 10.3390/medicina56050240

Baracchi F, Ingiosi AM, Raymond RM, Opp MR, 2011. Sepsis-induced alterations in sleep of rats. American Journal of Physiology - Regulatory Integrative and Comparative Physiology 301. 10.1152/ajpregu.00354.2011

Bast T, Pezze M, McGarrity S, 2017. Cognitive deficits caused by prefrontal cortical and hippocampal neural disinhibition. British Journal of Pharmacology. 10.1111/bph.13850

Bastarache JA, Smith K, Jesse JJ, Putz ND, Meegan JE, Bogart AM, Schaaf K, Ghosh S, Shaver CM, Ware LB, 2021. A two-hit model of sepsis plus hyperoxia causes lung permeability and inflammation. American Journal of Physiology-Lung Cellular and Molecular Physiology. 10.1152/ajplung.00227.2021

Bauer M, Coldewey SM, Leitner M, Löffler B, Weis S, Wetzker R, 2018. Deterioration of organ function as a hallmark in sepsis: The cellular perspective. Frontiers in Immunology 9, 1460. 10.3389/fimmu.2018.01460 [PubMed: 29997622]

Beyer MMS, Lonnemann N, Remus A, Latz E, Heneka MT, Korte M, 2020. Enduring Changes in Neuronal Function upon Systemic Inflammation Are NLRP3 Inflammasome Dependent. Journal of Neuroscience 40, 5480–5494. 10.1523/JNEUROSCI.0200-20.2020 [PubMed: 32499379]

Choi J, Kim SJ, Fujiyama T, Miyoshi C, Park M, Suzuki-Abe H, Yanagisawa M, Funato H, 2021. The Role of Reproductive Hormones in Sex Differences in Sleep Homeostasis and Arousal Response in Mice. Front Neurosci 15, 739236. 10.3389/fnins.2021.739236 [PubMed: 34621154]

Chou CH, Lee JT, Lin Chun Chieh, Sung YF, Lin Che Chen, Muo CH, Yang FC, Wen CP, Wang IK, Kao CH, Hsu CY, Tseng CH, 2017. Septicemia is associated with increased risk for dementia: A population-based longitudinal study. Oncotarget 8, 84300–84308. 10.18632/oncotarget.20899 [PubMed: 29137424]

Consoli David C., Jesse JJ, Klimo KR, Tienda AA, Putz ND, Bastarache JA, Harrison FE, 2020. A Cecal Slurry Mouse Model of Sepsis Leads to Acute Consumption of Vitamin C in the Brain. Nutrients 12, 911. 10.3390/nu12040911 [PubMed: 32224930]

Crosby G, Culley DJ, 2011. Surgery and anesthesia: Healing the body but harming the brain? Anesthesia and Analgesia. 10.1213/ANE.0b013e3182160431

Crosby G, Culley DJ, Marcantonio ER, 2010. Delirium: A cognitive cost of the comfort of procedural sedation in elderly patients? Mayo Clinic Proceedings. 10.4065/mcp.2009.0724

Deacon RM, 2006. Assessing nest building in mice. Nat Protoc 1, 1117–9. 10.1038/nprot.2006.170 [PubMed: 17406392]

Deacon RM, Rawlins JN, 2002. Learning impairments of hippocampal-lesioned mice in a paddling pool. Behavioral neuroscience 116, 472–8. [PubMed: 12049328]

Deacon RMJ, Croucher A, Rawlins JNP, 2002. Hippocampal cytotoxic lesion effects on species-typical behaviours in mice. Behavioural Brain Research 132, 203–213. 10.1016/S0166-4328(01)00401-6 [PubMed: 11997150]

Drouot X, Roche-Campo F, Thille AW, Cabello B, Galia F, Margarit L, D'Ortho MP, Brochard L, 2012. A new classification for sleep analysis in critically ill patients. Sleep Medicine 13, 7–14. 10.1016/j.sleep.2011.07.012 [PubMed: 22153778]

Ely EW, Bernard GR, Speroff T, Gautam S, Dittus R, May L, Truman B, Ely EW, Bernard GR, Gordon S, Margolin R, Inouye SK, Francis J, Hart RP, 2001. Delirium in mechanically ventilated patients: Validity and reliability of the Confusion Assessment Method for the intensive care unit (CAM-ICU). Journal of the American Medical Association 286, 2703–2710. 10.1001/jama.286.21.2703 [PubMed: 11730446]

Ely EW, Shintani A, Truman B, Speroff T, Gordon SM, Harrell FE, Inouye SK, Bernard GR, Dittus RS, 2004. Delirium as a Predictor of Mortality in Mechanically Ventilated Patients in the Intensive Care Unit. Journal of the American Medical Association 291, 1753–1762. 10.1001/jama.291.14.1753 [PubMed: 15082703]

Engel GL, Romano J, 1959. Delirium, a syndrome of cerebral insufficiency. Journal of Chronic Diseases 9, 260–277. 10.1016/0021-9681(59)90165-1 [PubMed: 13631039]

Field RH, Gossen A, Cunningham C, 2012. Prior pathology in the basal forebrain cholinergic system predisposes to inflammation-induced working memory deficits: Reconciling inflammatory and cholinergic hypotheses of delirium. Journal of Neuroscience 32, 6288–6294. 10.1523/JNEUROSCI.4673-11.2012 [PubMed: 22553034]

Gómez-Nieto R, Hormigo S, López DE, 2020. Prepulse Inhibition of the Auditory Startle Reflex Assessment as a Hallmark of Brainstem Sensorimotor Gating Mechanisms. Brain Sci 10, E639. 10.3390/brainsci10090639

Gould RW, Russell JK, Nedelcovych MT, Bubser M, Blobaum AL, Bridges TM, Newhouse PA, Lindsley CW, Conn PJ, Nader MA, Jones CK, 2020. Modulation of arousal and sleep/wake architecture by M1 PAM VU0453595 across young and aged rodents and nonhuman primates. Neuropsychopharmacology 45, 2219–2228. 10.1038/s41386-020-00812-7 [PubMed: 32868847]

Grahl JJ, Stollings JL, Rakhit S, Person AK, Wang L, Thompson JL, Pandharipande PP, Wesley Ely E, Patel MB, 2018. Antimicrobial exposure and the risk of delirium in critically ill patients 11 Medical and Health Sciences 1103 Clinical Sciences. Critical Care 22. 10.1186/s13054-018-2262-z

Hammer TB, Oranje B, Skimminge A, Aggernæs B, Ebdrup BH, Glenthøj B, Baaré W, 2013. Structural brain correlates of sensorimotor gating in antipsychotic-naive men with first-episode schizophrenia. Journal of Psychiatry and Neuroscience 38, 34–42. 10.1503/jpn.110129 [PubMed: 22687247]

Hedrick TP, Nobis WP, Foote KM, Ishii T, Chetkovich DM, Swanson GT, 2017. Excitatory Synaptic Input to Hilar Mossy Cells under Basal and Hyperexcitable Conditions. eNeuro 4. 10.1523/ENEURO.0364-17.2017

Hinson HE, Sheth KN, 2012. Manifestations of the hyperadrenergic state after acute brain injury. Current Opinion in Critical Care. 10.1097/MCC.0b013e3283513290

Hippensteel JA, Anderson BJ, Orfila JE, McMurtry SA, Dietz RM, Su G, Ford JA, Oshima K, Yang Y, Zhang F, Han X, Yu Y, Liu J, Linhardt RJ, Meyer NJ, Herson PS, Schmidt EP, 2019. Circulating heparan sulfate fragments mediate septic cognitive dysfunction. Journal of Clinical Investigation 129, 1779–1784. 10.1172/JCI124485 [PubMed: 30720464]

Hirsch LJ, Fong MWK, Leitinger M, LaRoche SM, Beniczky S, Abend NS, Lee JW, Wusthoff CJ, Hahn CD, Westover MB, Gerard EE, Herman ST, Haider HA, Osman G, Rodriguez-Ruiz A, Maciel CB, Gilmore EJ, Fernandez A, Rosenthal ES, Claassen J, Husain AM, Yoo JY, So EL, Kaplan PW, Nuwer MR, van Putten M, Sutter R, Drislane FW, Trinka E, Gaspard N, 2021. American Clinical Neurophysiology Society's Standardized Critical Care EEG Terminology: 2021 Version. Journal of clinical neurophysiology : official publication of the American Electroencephalographic Society 38, 1–29. 10.1097/WNP.0000000000000806 [PubMed: 33475321]

Hughes CG, Morandi A, Girard TD, Riedel B, Thompson JL, Shintani AK, Pun BT, Wesley Ely E, Pandharipande PP, 2013. Association between endothelial dysfunction and acute brain dysfunction during critical illness. Anesthesiology 118, 631–639. 10.1097/ALN.0b013e31827bd193 [PubMed: 23263016]

Illendula M, Osuru HP, Ferrarese B, Atluri N, Dulko E, Zuo Z, Lunardi N, 2020. Surgery, Anesthesia and Intensive Care Environment Induce Delirium-Like Behaviors and Impairment of Synaptic Function-Related Gene Expression in Aged Mice. Frontiers in Aging Neuroscience 12. 10.3389/fnagi.2020.542421

Iwashyna TJ, Ely EW, Smith DM, Langa KM, 2010. Long-term cognitive impairment and functional disability among survivors of severe sepsis. JAMA - Journal of the American Medical Association 304, 1787–1794. 10.1001/jama.2010.1553 [PubMed: 20978258]

Jacobson SA, Leuchter AF, Walter DO, 1993. Conventional and quantitative EEG in the diagnosis of delirium among the elderly. Journal of Neurology Neurosurgery and Psychiatry 56, 153–158. 10.1136/jnnp.56.2.153 [PubMed: 8437004]

Janus C, Flores AY, Xu G, Borchelt DR, 2015. Behavioral abnormalities in APPSwe/PS1dE9 mouse model of AD-like pathology: comparative analysis across multiple behavioral domains. Neurobiol Aging 36, 2519–2532. 10.1016/j.neurobiolaging.2015.05.010 [PubMed: 26089165]

Kamiński J, Brzezicka A, Gola M, Wróbel A, 2012. Beta band oscillations engagement in human alertness process. International Journal of Psychophysiology 85, 125–128. 10.1016/j.ijpsycho.2011.11.006 [PubMed: 22155528]

Kerchberger EV, Bastarache JA, Shaver CM, Nagata H, Brennan McNeil J, Landstreet SR, Putz ND, Kuang Yu W, Jesse J, Wickersham NE, Sidorova TN, Janz DR, Parikh CR, Siew ED, Ware LB, Eric Kerchberger V, Bastarache JA, Shaver CM, Nagata H, Brennan McNeil J, Landstreet SR, Putz ND, Kuang Yu W, Jesse J, Wickersham NE, Sidorova TN, Janz DR, Parikh CR, Siew ED, Ware LB, 2019. Haptoglobin-2 variant increases susceptibility to acute respiratory distress syndrome during sepsis. JCI Insight 4. 10.1172/jci.insight.131206

Kimchi E, Coughlin B, Cash S, 2017. Rodent models of delirium and encephalopathy: Behavioral and neurophysiological studies in aging (P5.090). Neurology 88.

Kimchi EY, Neelagiri A, Whitt W, Sagi AR, Ryan SL, Gadbois G, Groothuysen D, Westover MB, 2019. Clinical EEG slowing correlates with delirium severity and predicts poor clinical outcomes. Neurology 93, E1260–E1271. 10.1212/WNL.0000000000008164 [PubMed: 31467255]

Koehl M, Battle S, Meerlo P, 2006. Sex differences in sleep: the response to sleep deprivation and restraint stress in mice. Sleep 29, 1224–1231. 10.1093/sleep/29.9.1224 [PubMed: 17040010]

Koponen H, Partanen J, Pääkkönen A, Mattila E, Riekkinen PJ, 1989. EEG spectral analysis in delirium. Journal of Neurology, Neurosurgery and Psychiatry 52, 980–985. 10.1136/jnnp.52.8.980 [PubMed: 2795067]

Kotfis K, Williams Roberson S, Wilson JE, Dabrowski W, Pun BT, Ely EW, 2020. COVID-19: ICU delirium management during SARS-CoV-2 pandemic. Critical Care. 10.1186/s13054-020-02882-x

Kumari V, Gray JA, Geyer MA, Ffytche D, Soni W, Mitterschiffthaler MT, Vythelingum GN, Simmons A, Williams SCR, Sharma T, 2003. Neural correlates of tactile prepulse inhibition: A functional MRI study in normal and schizophrenic subjects. Psychiatry Research - Neuroimaging 122, 99–113. 10.1016/S0925-4927(02)00123-3

Leavitt ML, Trzepacz PT, Ciongoli K, 1994. Rat model of delirium: Atropine dose-response relationships. Journal of Neuropsychiatry and Clinical Neurosciences 6, 279–284. 10.1176/jnp.6.3.279 [PubMed: 7950352]

Li L, Du Y, Li N, Wu X, Wu Y, 2009. Top-down modulation of prepulse inhibition of the startle reflex in humans and rats. Neurosci Biobehav Rev 33, 1157–1167. 10.1016/j.neubiorev.2009.02.001 [PubMed: 19747594]

Lynch MA, 2004. Long-Term Potentiation and Memory. Physiological Reviews. 10.1152/physrev.00014.2003

Madsen GF, Bilenberg N, Cantio C, Oranje B, 2014. Increased prepulse inhibition and sensitization of the startle reflex in autistic children. Autism Research 7, 94–103. 10.1002/aur.1337 [PubMed: 24124111]

Mart MF, Williams Roberson S, Salas B, Pandharipande PP, Ely EW, 2020. Prevention and Management of Delirium in the Intensive Care Unit. Seminars in Respiratory and Critical Care Medicine. 10.1055/s-0040-1710572

Mazeraud A, Pascal Q, Verdonk F, Heming N, Chrétien F, Sharshar T, 2016. Neuroanatomy and Physiology of Brain Dysfunction in Sepsis. Clinics in Chest Medicine. 10.1016/j.ccm.2016.01.013

McGarrity S, Mason R, Fone KC, Pezze M, Bast T, 2017. Hippocampal neural disinhibition causes attentional and memory deficits. Cerebral Cortex 27, 4447–4462. 10.1093/cercor/bhw247 [PubMed: 27550864]

Meegan JE, Shaver CM, Putz ND, Jesse JJ, Landstreet SR, Lee HNR, Sidorova TN, Brennan McNeil J, Wynn JL, Cheung-Flynn J, Komalavilas P, Brophy CM, Ware LB, Bastarache JA, 2020. Cell-free hemoglobin increases inflammation, lung apoptosis, and microvascular permeability in murine polymicrobial sepsis. PLoS ONE 15, e0228727. 10.1371/journal.pone.0228727 [PubMed: 32012200]

Mena A, Ruiz-Salas JC, Puentes A, Dorado I, Ruiz-Veguilla M, De la Casa LG, 2016. Reduced prepulse inhibition as a biomarker of schizophrenia. Frontiers in Behavioral Neuroscience 10, 202. 10.3389/fnbeh.2016.00202 [PubMed: 27803654]

Miller AD, Ball AM, Bookstaver PB, Dornblaser EK, Bennett CL, 2011. Epileptogenic potential of carbapenem agents: Mechanism of action, seizure rates, and clinical considerations. Pharmacotherapy. 10.1592/phco.31.4.408

Moretti DV, Prestia A, Fracassi C, Binetti G, Zanetti O, Frisoni GB, 2012. Specific EEG changes associated with atrophy of hippocampus in subjects with mild cognitive impairment and Alzheimer's disease. International Journal of Alzheimer's Disease. 10.1155/2012/253153

Mulkey MA, Everhart DE, Kim S, Olson DWM, Hardin SR, 2019. Detecting delirium using a physiologic monitor. Dimensions of Critical Care Nursing 38, 241–247. 10.1097/DCC.0000000000000372 [PubMed: 31369442]

Nielsen RM, Urdanibia-Centelles O, Vedel-Larsen E, Thomsen KJ, Møller K, Olsen KS, Lauritsen AØ, Eddelien HS, Lauritzen M, Benedek K, 2019. Continuous EEG Monitoring in a Consecutive Patient Cohort with Sepsis and Delirium. Neurocritical Care 2019 32:1 32, 121–130. 10.1007/S12028-019-00703-W

O'Neill E, Griffin ÉW, O'Sullivan R, Murray C, Ryan L, Yssel J, Harkin A, Cunningham C, 2021. Acute neuroinflammation, sickness behavior and working memory responses to acute systemic LPS challenge following noradrenergic lesion in mice. Brain, Behavior, and Immunity 94, 357–368. 10.1016/j.bbi.2020.12.002 [PubMed: 33307172]

Opp MR, George A, Ringgold KM, Hansen KM, Bullock KM, Banks WA, 2015. Sleep fragmentation and sepsis differentially impact blood-brain barrier integrity and transport of tumor necrosis factor-α in aging. Brain, Behavior, and Immunity 50, 259–265. 10.1016/j.bbi.2015.07.023 [PubMed: 26218294]

Palanca BJA, Wildes TS, Ju YS, Ching S, Avidan MS, 2017. Electroencephalography and delirium in the postoperative period. British Journal of Anaesthesia. 10.1093/bja/aew475

Pandharipande PP, Girard TD, Jackson JC, Morandi A, Thompson JL, Pun BT, Brummel NE, Hughes CG, Vasilevskis EE, Shintani AK, Moons KG, Geevarghese SK, Canonico A, Hopkins RO, Bernard GR, Dittus RS, Ely EW, 2013. Long-Term Cognitive Impairment after Critical Illness. New England Journal of Medicine 369, 1306–1316. 10.1056/nejmoa1301372 [PubMed: 24088092]

Paul KN, Dugovic C, Turek FW, Laposky AD, 2006. Diurnal sex differences in the sleep-wake cycle of mice are dependent on gonadal function. Sleep 29, 1211–1223. 10.1093/sleep/29.9.1211 [PubMed: 17040009]

Pun BT, Badenes R, Heras La Calle G, Orun OM, Chen W, Raman R, Simpson BGK, Wilson-Linville S, Hinojal Olmedillo B, Vallejo de la Cueva A, van der Jagt M, Navarro Casado R, Leal Sanz P, Orhun G, Ferrer Gómez C, Núñez Vázquez K, Piñeiro Otero P, Taccone FS, Gallego Curto E, Caricato A, Woien H, Lacave G, O'Neal HR, Peterson SJ, Brummel NE, Girard TD, Ely EW, Pandharipande PP, Creteur J, Bogossian EG, Peluso L, González-Seguel F, Hidalgo-Cabalín V, Carreño-Montenegro P, Rojas V, Tobar E, Ramírez-Palma A, Herrera-Davis K, Ferré A, Legriel S, Godet T, Fraisse U, Gonçalves B, Mazeraud A, Tzimou M, Rasulo F, Beretta S, Marchesi M, Robba C, Battaglini D, Pelosi P, Mazzeo AT, Noto A, Servillo G, Marra A, Cutuli SL, Pintaudi G, Stival E, Tanzarella ES, Roman-Pognuz E, Concetta Massaro CM, Elhadi M, Smit L, Olasveengen T, Pereira IJ, Teixeira CM, Santos A, Valente M, Granja C, Pereia R, Silva J, Furquet B, García Simón M, Godoy Torres DA, Monleón B, Morcillo E, Romero N, Serrano A, Torrico Sánchez S, Pérez Caballero FL, Peña Luna I, Baeza Gómez I, Calizaya Vargas M, Morillas Pérez J, Carrasco Gómez G, Molina Latorre R, Moya Gutiérrez S, Barón Barrera IP, Delgado Palacios C, García

Góngora B, Labrador Romero L, Galarza L, Catalán-Monzón I, Rodriguez-Martínez E, Murcia Gubianas C, Bellès A, Rodriguez Delgado ME, Caballero J, Morales D, Pujol A, Rubio J, Álvarez Torres E, Carvajal Revuelta E, de la Calle Gil I, Fernández Tomás B, Gallego Rodríguez B, González Serrano M, LaTorre Andreu P, Pérez Lucendo A, Abril Palomares E, González González E, Martín Delgado MC, Muñoz De Cabo C, Aznar PT, Calvo CA, Garutti I, Higuero F, Martínez-Gascueña D, Maseda E, Insausti I, Montero Feijoo A, Suarez-de-la-Rica A, Del Moral Barbudo B, García Blanco-Traba Y, Giménez Santamarina MC, Gonzalo Millán A, Llorente Damas S, Pestaña Lagunas D, Reyes García I, Ruiz Perea A, Ortega Guerrero Á, Mármol Cubillo MJ, Díaz Muñoz D, García de Castrillón i Ramal S, Andorrà Sunyer X, Noci Moreno M de las N, Pérez Manrique RM, del Campo Molina E, Martínez Quintana ME, Fernandez-Gonzalo S, Gomà Fernández G, Navarra-Ventura G, Baró Serra A, Fuster C, Plans Galván O, Gil-Castillejos D, Dalorzo González M, Morán Gallego FJ, Paredes Borrachero I, Rodríguez Villamizar P, Romeu Prieto J, Sánchez Carretero MJ, Gallardo Sánchez S, Bustos Molina F, García Pérez ML, Castello-Mora P, Puig J, Sanchis-Martin MR, Sanchis-Veryser CA, Vicente-Fernández MP, Zaragoza R, Lizama L, Torres I, Álvarez C, Ramírez P, Martin Cerezuela M, Montero MJ, García Cantos J, Valls P, Aretxabala Cortajarena N, García Domelo P, González Cubillo L, Martín Martínez M, Pérez Francisco I, Poveda Hernández Y, Quintano Rodero A, Rodriguez Nuñez C, Siegemund M, Estermann A, Zellweger N, Ben Saida I, Boussarsar M, Esen F, Ergin Özcan P, Berkey C, Harb C, Tandy MH, Morgan E, Shephard K, Hyzy RC, Kenes M, Nelson K, Hosse RE, Vance KM, Austin CA, Lerner A, Sanders E, Balk RA, Bennett DA, Vogel AR, Chowdhury L, Devulapally K, Woodham M, Cohen S, Patel N, Kuza CM, Sing M, Roberson S, Drumright K, Sehgal S, LaHue SC, Douglas VC, Sarwal A, 2021. Prevalence and risk factors for delirium in critically ill patients with COVID-19 (COVID-D): a multicentre cohort study. The Lancet Respiratory Medicine 9, 239–250. 10.1016/S2213-2600(20)30552-X [PubMed: 33428871]

Remick DG, 2007. Pathophysiology of sepsis. American Journal of Pathology 170, 1435–1444. 10.2353/ajpath.2007.060872 [PubMed: 17456750]

Rengel KF, Hayhurst CJ, Pandharipande PP, Hughes CG, 2019. Long-term Cognitive and Functional Impairments After Critical Illness. Anesthesia and analgesia. 10.1213/ANE.0000000000004066

Ritzel RM, Li Y, He J, Khan N, Doran SJ, Faden AI, Wu J, 2020. Sustained neuronal and microglial alterations are associated with diverse neurobehavioral dysfunction long after experimental brain injury. Neurobiol Dis 136, 104713. 10.1016/j.nbd.2019.104713 [PubMed: 31843705]

Robbins TW, 2002. The 5-choice serial reaction time task: behavioural pharmacology and functional neurochemistry. Psychopharmacology (Berl) 163, 362–380. 10.1007/s00213-002-1154-7 [PubMed: 12373437]

Robbins TW, Muir JL, Killcross AS, Pretsell DO, 1993. Methods for Assessing attention and stimulus control in the rat., in: Behavioral Neuroscience, a Practical Approach. Oxford University Press, New York, pp. 13–47.

Roberson SW, Azeez NA, Taneja R, Pun BT, Pandharipande PP, Jackson JC, Ely EW, 2020. Quantitative EEG During Critical Illness Correlates With Patterns of Long-Term Cognitive Impairment: https://doi.org/10.1177/1550059420978009. 10.1177/1550059420978009

Rudd KE, Johnson SC, Agesa KM, Shackelford KA, Tsoi D, Kievlan DR, Colombara DV, Ikuta KS, Kissoon N, Finfer S, Fleischmann-Struzek C, Machado FR, Reinhart KK, Rowan K, Seymour CW, Watson RS, West TE, Marinho F, Hay SI, Lozano R, Lopez AD, Angus DC, Murray CJL, Naghavi M, 2020. Global, regional, and national sepsis incidence and mortality, 1990–2017: analysis for the Global Burden of Disease Study. The Lancet 395, 200–211. 10.1016/S0140-6736(19)32989-7

Sasannejad C, Ely EW, Lahiri S, 2019. Long-term cognitive impairment after acute respiratory distress syndrome: A review of clinical impact and pathophysiological mechanisms. Critical Care. 10.1186/s13054-019-2626-z

Satapathy SK, Dehuri S, Jagadev AK, Mishra S, 2019. EEG Brain Signal Classification for Epileptic Seizure Disorder Detection, EEG Brain Signal Classification for Epileptic Seizure Disorder Detection. Elsevier. 10.1016/c2018-0-01888-5

Schwalm MT, Pasquali M, Miguel SP, Dos Santos JPA, Vuolo F, Comim CM, Petronilho F, Quevedo J, Gelain DP, Moreira JCF, Ritter C, Dal-Pizzol F, 2014. Acute brain inflammation and oxidative damage are related to long-term cognitive deficits and markers of neurodegeneration in sepsis-survivor rats. Molecular Neurobiology. 10.1007/s12035-013-8526-3

Semmler A, Frisch C, Debeir T, Ramanathan M, Okulla T, Klockgether T, Heneka MT, 2007. Long-term cognitive impairment, neuronal loss and reduced cortical cholinergic innervation after recovery from sepsis in a rodent model. Experimental Neurology 204, 733–740. 10.1016/j.expneurol.2007.01.003 [PubMed: 17306796]

Sessler CN, Gosnell MS, Grap MJ, Brophy GM, O'Neal PV, Keane KA, Tesoro EP, Elswick RK, 2002. The Richmond Agitation-Sedation Scale: Validity and reliability in adult intensive care unit patients. American Journal of Respiratory and Critical Care Medicine 166, 1338–1344. 10.1164/rccm.2107138 [PubMed: 12421743]

Shaver CM, Paul MG, Putz ND, Landstreet SR, Kuck JL, Scarfe L, Skrypnyk N, Yang H, Harrison FE, de Caestecker MP, Bastarache JA, Ware LB, 2019. Cell-free hemoglobin augments acute kidney injury during experimental sepsis. American Journal of Physiology-Renal Physiology 317, F922–F929. 10.1152/ajprenal.00375.2018 [PubMed: 31364379]

Shinozaki G, Bormann NL, Chan AC, Zarei K, Sparr NA, Klisares MJ, Jellison SS, Heinzman JT, Dahlstrom EB, Duncan GN, Gaul LN, Wanzek RJ, Cramer EM, Wimmel CG, Sabbagh S, Yuki K, Weckmann MT, Yamada T, Karam MD, Noiseux NO, Shinozaki E, Cho HR, Lee S, Cromwell JW, 2019. Identification of Patients With High Mortality Risk and Prediction of Outcomes in Delirium by Bispectral EEG. J Clin Psychiatry 80, 19m12749. 10.4088/JCP.19m12749

Shinozaki G, Chan AC, Sparr NA, Zarei K, Gaul LN, Heinzman JT, Robles J, Yuki K, Chronis TJ, Ando T, Wong T, Sabbagh S, Weckmann MT, Lee S, Yamada T, Karam MD, Noiseux NO, Shinozaki E, Cromwell JW, 2018. Delirium detection by a novel bispectral electroencephalography device in general hospital. Psychiatry Clin Neurosci 72, 856–863. 10.1111/pcn.12783 [PubMed: 30246448]

Singer M, Deutschman CS, Seymour CW, Shankar-Hari M, Annane D, Bauer M, Bellomo R, Bernard GR, Chiche J-D, Coopersmith CM, Hotchkiss RS, Levy MM, Marshall JC, Martin GS, Opal SM, Rubenfeld GD, van der Poll T, Vincent J-L, Angus DC, 2016. The Third International Consensus Definitions for Sepsis and Septic Shock (Sepsis-3). JAMA 315, 801–810. 10.1001/jama.2016.0287 [PubMed: 26903338]

Skelly DT, Griffin ÉW, Murray CL, Harney S, O'Boyle C, Hennessy E, Dansereau M-A, Nazmi A, Tortorelli L, Rawlins JN, Bannerman DM, Cunningham C, 2019. Acute transient cognitive dysfunction and acute brain injury induced by systemic inflammation occur by dissociable IL-1-dependent mechanisms. Molecular Psychiatry 24, 1533. 10.1038/S41380-018-0075-8 [PubMed: 29875474]

Slooter AJC, Otte WM, Devlin JW, Arora RC, Bleck TP, Claassen J, Duprey MS, Ely EW, Kaplan PW, Latronico N, Morandi A, Neufeld KJ, Sharshar T, MacLullich AMJ, Stevens RD, 2020. Updated nomenclature of delirium and acute encephalopathy: statement of ten Societies. Intensive Care Medicine 46, 1020–1022. 10.1007/s00134-019-05907-4 [PubMed: 32055887]

Steele AM, Starr ME, Saito H, 2017. Late Therapeutic Intervention with Antibiotics and Fluid Resuscitation Allows for a Prolonged Disease Course with High Survival in a Severe Murine Model of Sepsis. Shock 47, 726–734. 10.1097/SHK.0000000000000799 [PubMed: 27879561]

Trzepacz PT, Leavitt M, Ciongoli K, 1992. An Animal Model for Delirium. Psychosomatics 33, 404–415. 10.1016/S0033-3182(92)71945-8 [PubMed: 1461966]

Van Lier H, Drinkenburg WHIM, Van Eeten YJW, Coenen AML, 2004. Effects of diazepam and zolpidem on EEG beta frequencies are behavior-specific in rats. Neuropharmacology 47, 163–174. 10.1016/j.neuropharm.2004.03.017 [PubMed: 15223295]

Velagapudi R, Subramaniyan S, Xiong C, Porkka F, Rodriguiz RM, Wetsel WC, Terrando N, 2019. Orthopedic Surgery Triggers Attention Deficits in a Delirium-Like Mouse Model. Front Immunol 10, 2675. 10.3389/fimmu.2019.02675 [PubMed: 31911786]

Walker J, Dixit S, Saulsberry A, May J, Harrison F, Dis Author manuscript N, 2017. Reversal of high fat diet-induced obesity improves glucose tolerance, inflammatory response, β-amyloid accumulation and cognitive decline in the APP/PSEN1 mouse model of Alzheimer's disease HHS Public Access Author manuscript. Neurobiol Dis 100, 87–98. 10.1016/j.nbd.2017.01.004 [PubMed: 28108292]

Watson PL, Pandharipande P, Gehlbach BK, Thompson JL, Shintani AK, Dittus BS, Bernard GR, Malow BA, Ely EW, 2013. Atypical sleep in ventilated patients: Empirical electroencephalography

findings and the path toward revised ICU sleep scoring criteria. Critical Care Medicine 41, 1958–1967. 10.1097/CCM.0b013e31828a3f75 [PubMed: 23863228]

Wilcox JM, Consoli DC, Tienda AA, Dixit S, Buchanan RA, May JM, Nobis WP, Harrison FE, 2021a. Altered synaptic glutamate homeostasis contributes to cognitive decline in young APP/PSEN1 mice. Neurobiology of Disease 158, 105486. 10.1016/j.nbd.2021.105486 [PubMed: 34450329]

Wilcox JM, Consoli DC, Tienda AA, Dixit S, Buchanan RA, May JM, Nobis WP, Harrison FE, 2021b. Altered synaptic glutamate homeostasis contributes to cognitive decline in young APP/PSEN1 mice. Neurobiol Dis 158, 105486. 10.1016/j.nbd.2021.105486 [PubMed: 34450329]

Wolters AE, Slooter AJC, Van Der Kooi AW, Van Dijk D, 2013. Cognitive impairment after intensive care unit admission: A systematic review. Intensive Care Medicine. 10.1007/s00134-012-2784-9

Yamanashi T, Malicoat JR, Steffen KT, Zarei K, Li R, Purnell BS, Najafi A, Saito K, Singh U, Toth BA, Lee S, Dailey ME, Cui H, Kaneko K, Cho HR, Iwata M, Buchanan GF, Shinozaki G, 2021a. Bispectral EEG (BSEEG) quantifying neuro-inflammation in mice induced by systemic inflammation: A potential mouse model of delirium. J Psychiatr Res 133, 205–211. 10.1016/j.jpsychires.2020.12.036 [PubMed: 33360427]

Yamanashi T, Marra PS, Crutchley KJ, Wahba NE, Malicoat JR, Sullivan EJ, Akers CC, Nicholson CA, Herrmann FM, Karam MD, Noiseux NO, Kaneko K, Shinozaki E, Iwata M, Cho HR, Lee S, Shinozaki G, 2021b. Mortality among patients with sepsis associated with a bispectral electroencephalography (BSEEG) score. Sci Rep 11, 14211. 10.1038/s41598-021-93588-9 [PubMed: 34244577]

Yuan D, Liu C, Wu J, Hu B, 2018. Nest-building activity as a reproducible and long-term stroke deficit test in a mouse model of stroke. Brain Behav 8, e00993. 10.1002/brb3.993 [PubMed: 30106254]

Zampieri FG, Park M, Machado FS, Azevedo LCP, 2011. Sepsis-associated encephalopathy: Not just delirium. Clinics. 10.1590/S1807-59322011001000024

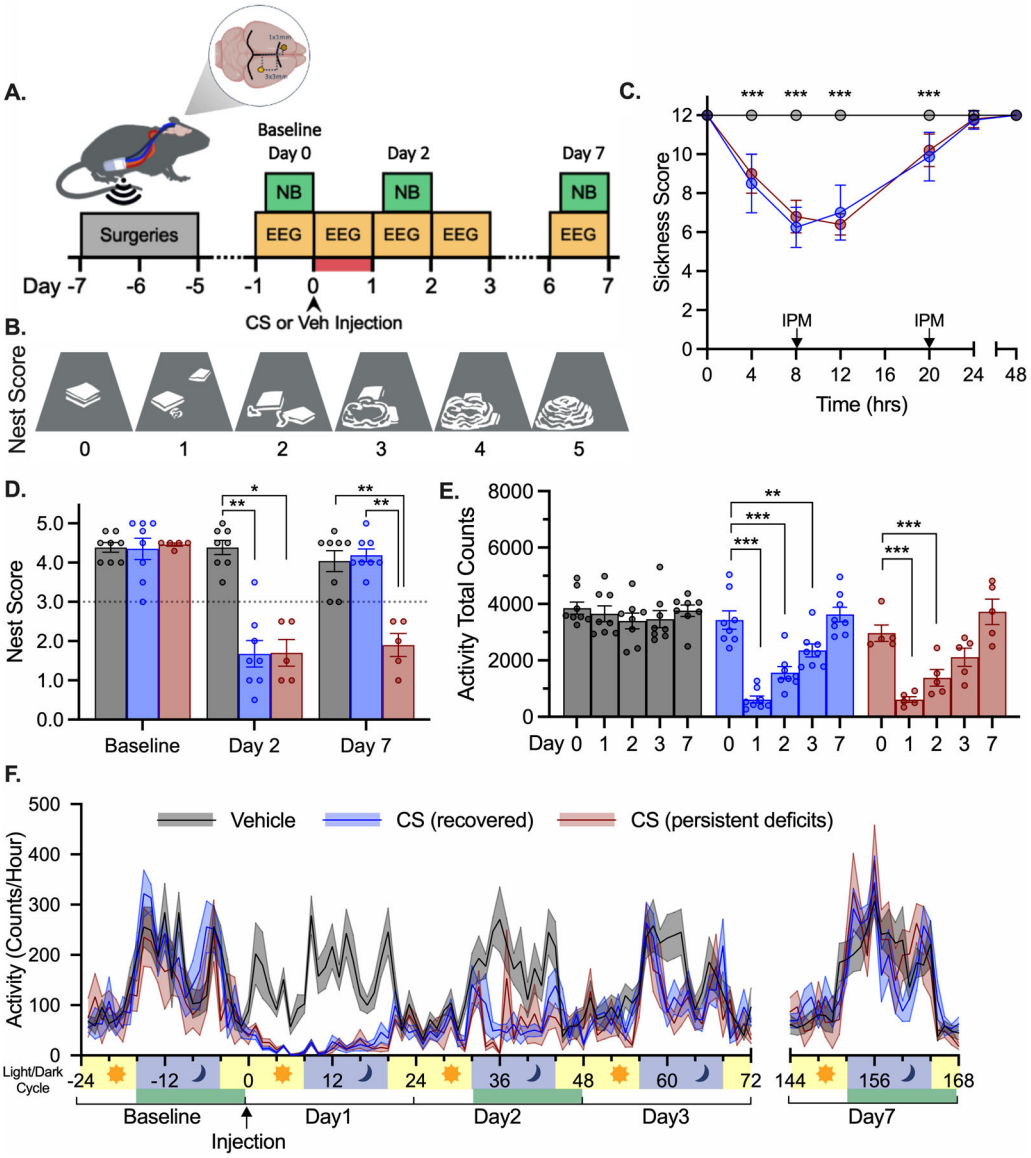

Figure 1.

Nest building and activity changes following sepsis. **(A)** EEG and behavior experimental timeline. Nest building (NB) task shown in green boxes was performed at baseline and on Days 2 and 7 following the illness period highlighted in red. Telemetry data were recorded in 24-hour increments as indicated in yellow boxes. For panels C-F CS-treated animals are divided into fully recovered (blue) and persistent impaired (red) based on nest building performance as shown in panel D. **(B)** Illustrations of nests representing a range of scores in order of increasing complexity, cage floor shown in grey, nestlet material in white. **(C)** Clinical Sickness Scores. IPM – imipenem (i.p. 1.5 mg/300 cc saline). **(D)** Nest scores following CS treatment and separation into groups based on performance on Day 7. **(E)** Total activity counts per day. **(F)** Activity counts per hour shown with light/dark phase of light cycle. Nest building task performed during times highlighted in green. ***p<0.001, **p<0.01, *p<0.05 both CS groups different from vehicle-treated, or as marked.

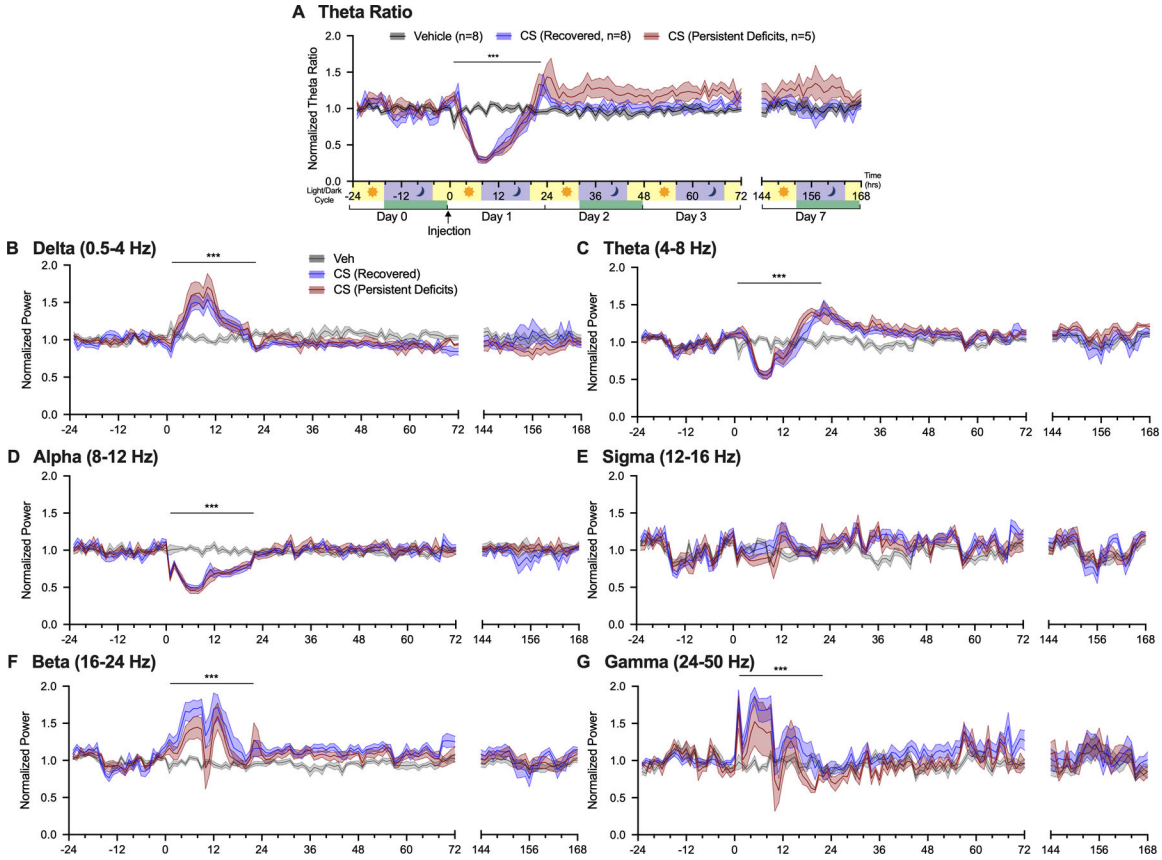

Figure 2.

CS-induced changes across EEG power bands. Average normalized theta ratio (**A**) and normalized power per hour for (**B**) delta (0.5–4 Hz), (**C**) theta (4–8 Hz), (**D**) alpha (8–12 Hz), (**E**) sigma (12–16 Hz), (**F**) beta (16–24 Hz), and (**G**) gamma (25–50 Hz). ***p<0.001 vehicle vs. all CS treated animals.

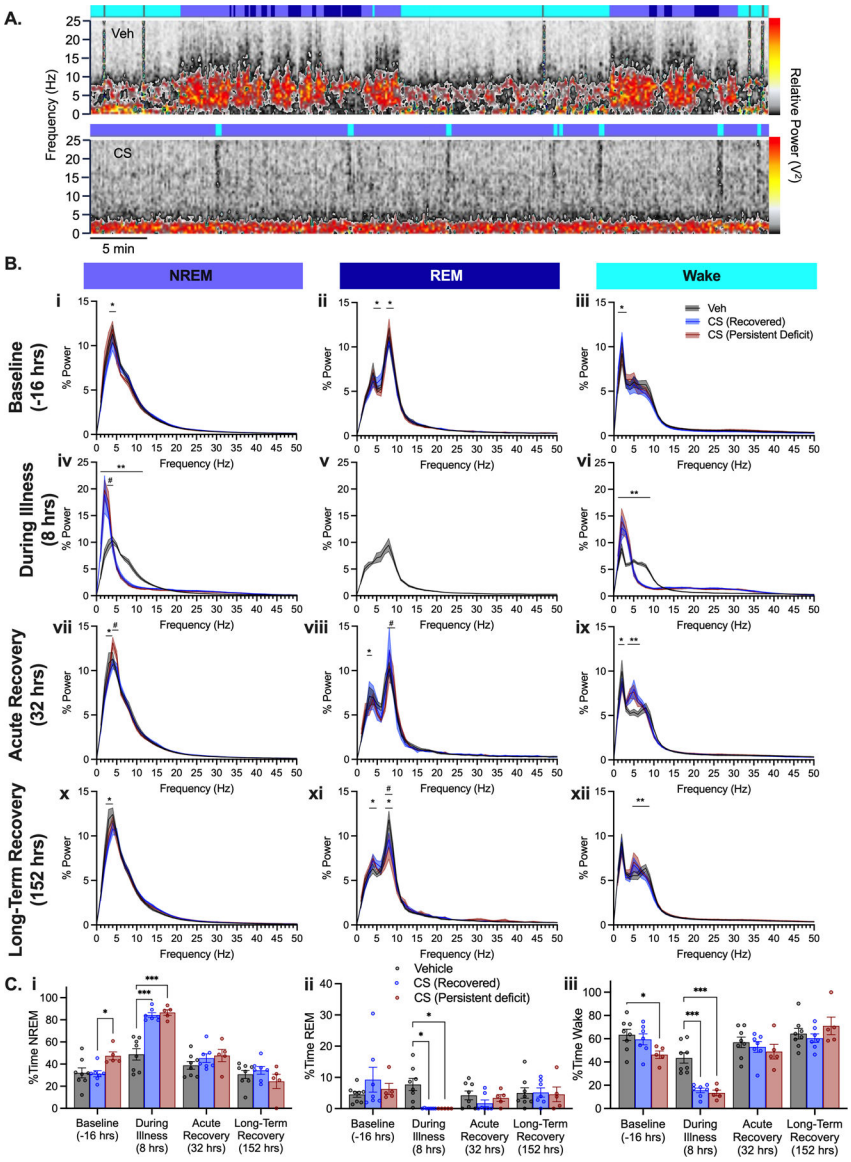

Figure 3.

Analysis of sleep patterns. (**A**) Representative one-hour spectral periodograms for individual mice treated with Vehicle (top) and CS (bottom) groups 8 hours following injection. Power 'scale' (red/yellow/grey) is equivalent for both top and bottom panels. Top colored ribbons indicate scored sleep stage for each 10 second epoch: blue – NREM sleep, dark blue – REM sleep, cyan – wake, gray – artifact/excluded. (**B**) Periodograms within sleep stages NREM sleep (left), REM sleep (middle) and wake (right) at baseline (**i-iii**), during illness (**iv-vi**), acute recovery (**vii-ix**), and long-term recovery (**x-xii**). (**C**) Duration spent in each sleep stage across scored timepoints. ***p<0.001, **p<0.01, *p<0.05 CS vs Veh; #p<0.01 CS Recovered vs. CS Persistent Deficits

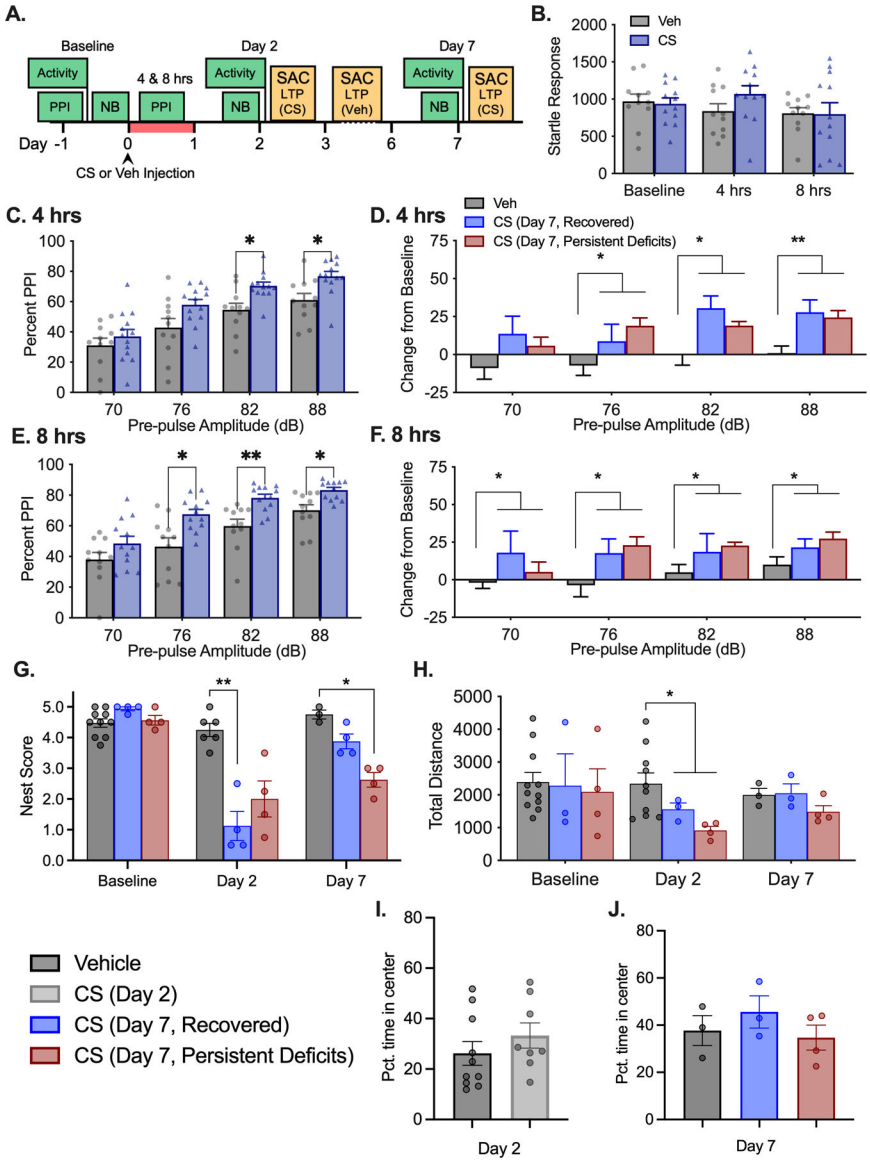

Figure 4.

Increased PPI during illness. (**A**) Experimental timeline. Nest building (NB), Pre-pulse inhibition of the startle response (PPI), and locomotor activity tasks were performed at timepoints indicated by green boxes. After NB scoring, CS treated mice were euthanized for LTP recording on Days 2 and 7 while vehicle treated mice were distributed between Days 2–7 as indicated in yellow boxes. Illness period is highlighted in red. Data collapsed into CS (all treated mice) and vehicle groups for initial analysis: **(B)** Startle response during 120 dB startle only trial. (**C**) PPI at 4 hours and (**E**) 8 hours post injection comparing all CS to Veh. Data were separated post-hoc according to differential nest building outcome on day 7: (**D**) PPI change from baseline at 4 hours and (**F**) 8 hours split by NB groups. (**G**) NB scores for each group prior to SAC for LTP recording. (**H**) Total locomotor activity during 30 min open field exploration task. **(I)** Pct. Time spent in center of locomotor activity chambers at 2 days

and **(J)** 7 days post CS injection. *, ** p's<0.05, 0.001 different from vehicle treated mice, as marked.

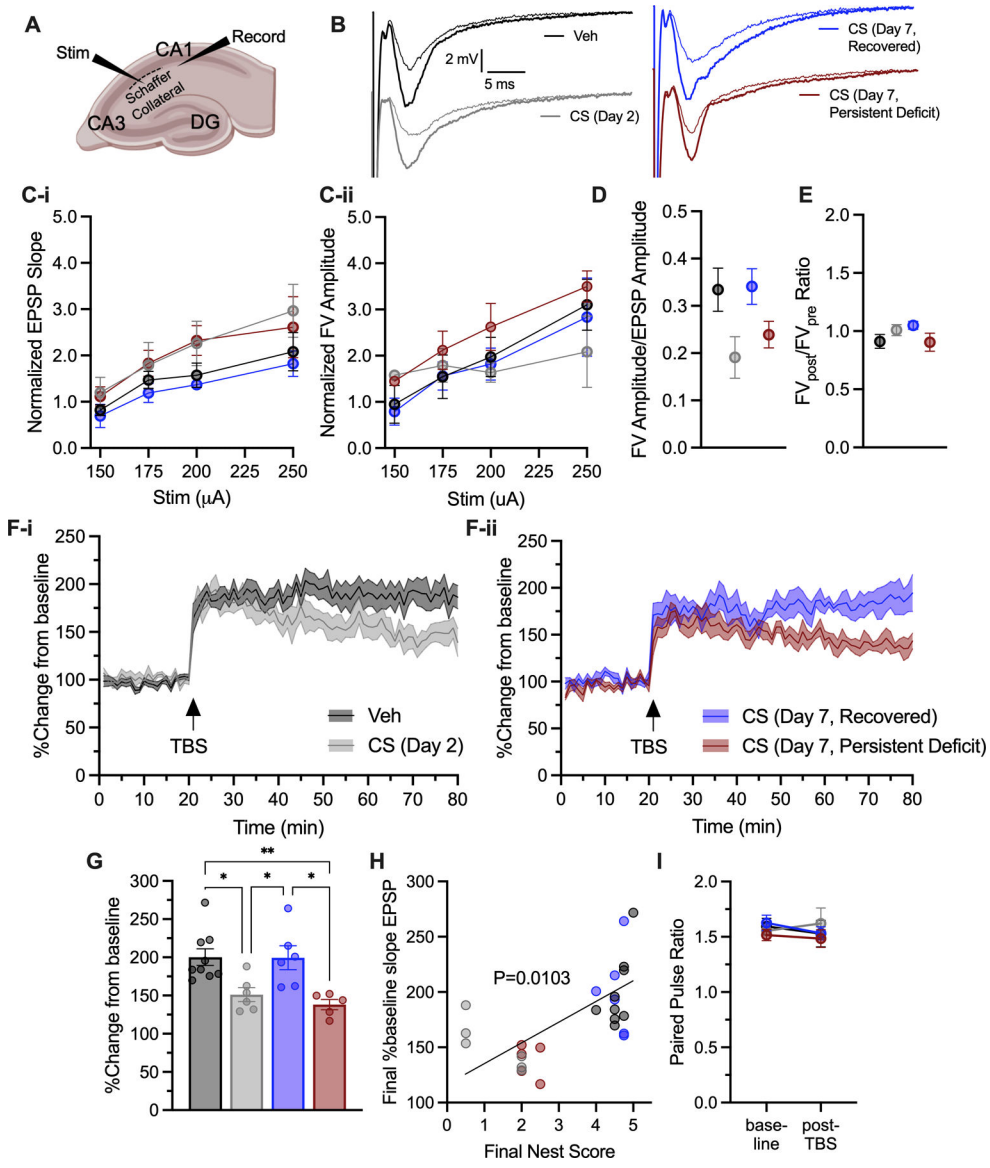

Figure 5.

Evaluation of long-term potentiation (LTP). (**A**) Stimulation and recording setup. (**B**) Representative EPSP traces after first pulse prior to (thin line) and post (thick line) TBS. (**C**) Input-output curves. (**D**) Fiber volley to EPSP ratio. (**E**) Fiber volley ratio pre/post TBS. (**F**) EPSP slope percent change from baseline and (**G**) final EPSP slope percent change from baseline in last 5 min. (**H**) Correlation with nest building. (**I**) Paired pulse ratio. TBS – theta burst stimulation.

Table 1.

Nest building behavioral task scoring criteria.

Nest Site	+0 No site	+0.5 Moved	+1 Clear site		
Percent of Nestlet Shredded	+0 <25%	+0.5 25%	+1 50%	+1.5 75%	+2 100%
	+1 Un-shredded nestlet utilized structurally as wall or roof				
Nest Height	+0 Flat	+0.5 Low	+1 Medium	+1.5 Med-High	+2 Dome